DEVELOPMENTAL DYNAMICS 241:1525–1544, 2012

RESEARCH ARTICLE

Developmental Dynamics

Mapping Differentiation Kinetics in the Mouse Retina Reveals an Extensive Period of Cell Cycle Protein Expression in Post-Mitotic Newborn Neurons

Marek Pacal[1,2] and Rod Bremner[1,2,3]*

Background: Knowledge of gene expression kinetics around neuronal cell birth is required to dissect mechanisms underlying progenitor fate. Here, we timed cell cycle and neuronal protein silencing/induction during cell birth in the developing murine retina. Results: The pan-cell cycle markers Pcna and Mcm6 were present in the post-mitotic ganglion cell layer. Although confined to the neuroblastic layer (NBL), 6–7% of Ki67$^+$ cells lacked six progenitor/cell cycle markers, and expressed neuronal markers. To define protein extinction/induction timing, we defined G2/M length throughout retinogenesis, which was typically 1–2 h, but <10% cells took double this time. BrdU-chase analyses revealed that at E12.5, Tubb3 (Tuj1) appeared at M-phase, followed by Calb2 and Dcx at ~2 h, Elavl2/3/4 at ~4 h, and Map2 at ~6 h after cell birth, and these times extended with embryonic age. Strikingly, Ki67 was not extinguished until up to a day after cell cycle exit, coinciding with exit from the NBL and induction of late markers such as Map1b/Uchl1/Rbfox3. Conclusions: A minor population of progenitors transits slowly through G2/M and, most importantly, some cell cycle proteins are retained for an unexpectedly long period in post-mitotic neurons. The high-resolution map of cell birth kinetics reported here provides a framework to better define mechanisms that regulate neurogenesis. *Developmental Dynamics 241:1525–1544, 2012.* © 2012 Wiley Periodicals, Inc.

Key words: retinal development; cell cycle length; G2/M; neuronal birth; neuronal marker induction; Ki67

Key findings:

- The pan cell cycle markers Pcna, Mcm6, and Ki67 are detectable beyond cell birth in post-mitotic neurons.
- Ki67 is not extinguished until 10–22 h after final mitosis, coincident with the migration of newborn ganglion and amacrine cells out of the neuroblastic layer.
- Timing between cell birth and induction of neuronal markers or disappearance of Ki67 lengthens across development.
- Typical G2/M extends from ~1 h at mouse embryonic day 12.5 to ~2 h by birth, but in a small fraction of progenitors it is double these lengths.

Accepted 18 July 2012

INTRODUCTION

Development requires careful coordination of proliferation, cell cycle exit, and differentiation. Defining the associated molecular cascade of gene silencing and activation events is essential to understand the mechanisms that underlie the switch from progenitor proliferation to

[1]Genetics and Development Division, Toronto Western Research Institute, University Health Network, Toronto, Canada
[2]Department of Ophthalmology and Vision Sciences, Department of Laboratory Medicine and Pathobiology, University of Toronto, Toronto, Canada
[3]Samuel Lunenfeld Research Institute, Mount Sinai Hospital, Toronto, Canada
Grant sponsor: CIHR; Grant number: MOP-74570; Grant sponsor: Foundation Fighting Blindness Canada; Grant number: 531524.
***Correspondence to: Rod Bremner, Toronto Western Research Institute, 399 Bathurst Street, Toronto, ON, Canada M5T 2S8. E-mail: rbremner@uhnres.utoronto.ca**

DOI 10.1002/dvdy.23840
Published online 13 August 2012 in Wiley Online Library (wileyonlinelibrary.com).

post-mitotic differentiation. The retina is an ideal tissue to dissect this process as it is a relatively simple, well-studied central nervous system (CNS) tissue, and is not essential for viability. Many antibodies have been generated that detect proteins in specific retinal cell types, and these are often used in combination with cell cycle markers to distinguish progenitors from differentiating or mature neurons. Nevertheless, the exact timing with which these neuronal proteins are induced relative to final mitosis has, in general, not been defined rigorously, nor is it clear if the kinetics adjust over developmental time. Moreover, it is assumed that cell cycle markers are unique to progenitors, but the exact time at which they are extinguished is unclear.

Initially, the embryonic mouse retina consists of dividing progenitors, but around embryonic day 11 (E11) cells in this neuroblastic layer (NBL) begin to exit the cell cycle and differentiate into ganglion cells (Fig. 1A). Mitosis occurs on the apical (outer) surface, and daughter neurons migrate to the basal (inner) surface of the tissue where they terminally differentiate and generate the ganglion cell layer (GCL). Murine ganglion cells are generated between embryonic day E11 and post-natal day 0 (P0), although most are born between E12–16 (Hinds and Hinds, 1974; Drager, 1985; Young, 1985a). Ganglion cell generation overlaps with that of other early born neurons, including horizontal, cone, and amacrine cells. The complete GCL contains a ~1:1 mixture of ganglion and amacrine neurons, as well as a few astrocytes that migrate into the retina along the optic nerve beyond P0. We studied the expression of several markers that are present in ganglion cells and/or other early born neurons (Table 1) as well as various cell cycle proteins (Table 2). Unexpectedly, we observed that the classic pan cell cycle marker Ki67 as well as the DNA polymerase δ/ϵ subunit Pcna and the DNA replication licensing factor Mcm6 were expressed in post-mitotic neurons. Ki67 is a nuclear protein mainly associated with cell proliferation (Endl and Gerdes, 2000). However, Ki67 is also required for the expression of rRNA in the nucleolus (Bullwinkel et al., 2006; Rahmanzadeh et al., 2007), but, interestingly, can also be detected in the nucleoli of post-mitotic cells (Bullwinkel et al., 2006). Our finding of cell cycle proteins in post-mitotic neurons led us to characterize more throughly when, relative to final mitosis, cell cycle and differentiation markers are extinguished or activated, respectively.

RESULTS

Ki67, But Not Pcna or Mcm6, Is Confined to the NBL

Ki67 and Pcna are used widely to mark all phases of the cell cycle. A more recent study has also highlighted the utility of Mcm6 as a pan-cell cycle marker in the retina (Barton and Levine, 2008). The latter study also noted that, based on flow cytometry cell cycle analysis, both Pcna and Mcm6 are also found in a significant proportion of cells with 2n DNA content, which may be in G1 or G0 (Barton and Levine, 2008). Another study found that the expression of both Pcna and Mcm6 mRNAs extends beyond progenitors into the ganglion and amacrine neuronal populations (Trimarchi et al., 2008), although whether this reflects protein expression is unclear. We found many $Mcm6^+$ cells, and to a lesser extent $Pcna^+$ cells, in the INBL and the forming GCL where post-mitotic ganglion neurons are found in the early embryonic retina (Fig. 1B). In comparison, $Ki67^+$ cells did not extend as far into the INBL as Mcm6 or Pcna, although there were occasional faintly labeled cells that marginally encroached into the forming GCL (Fig. 1B). We concluded that some G0 neurons retain Mcm6 and Pcna, and thus next scrutinized whether $Ki67^+$ cells, confined to the NBL, may include post-mitotic differentiating cells.

Ki67 Labels All Phases of the Cell Cycle in All Progenitors

To more comprehensively define Ki67 staining pattern, we first examined the assumption that it co-labels all phases of the cell cycle in retinal progenitors (Fig. 1C). A short pulse of BrdU is commonly used to label S-phase progenitors. The expression of Ccna2 (Cyclin A2) and Ccnb1 (Cyclin B1) can be used to visualize progenitors in the G2 /M-phases (Barton and Levine, 2008). Both cyclins can be detected in progenitor processes and display perinuclear and nuclear staining in G2 cells near the apical surface (Barton and Levine, 2008). Finally, phosphorylation of histone H3 on Ser 10 (PH3) accompanies chromosome condensation at the beginning of mitosis (Hendzel et al., 1997). In cultured cells, anti-PH3 antibodies detect strong nuclear staining from the beginning of prophase to telophase (Prigent and Dimitrov, 2003; Li et al., 2005) and are widely used to detect mitotic progenitors. Ki67 co-localized with all of four of these markers (30-min BrdU pulse, Ccna2, Ccnb1, and PH3) at multiple time points during retinal development (Fig. 1D, Table 3). These data confirm that Ki67 marks all progenitors throughout the cell cycle.

A Subset of $Ki67^+$ Cells Lack the Pan-Cell Cycle Markers Vsx2 and Ccnd1

If Ki67 is detectable in post-mitotic differentiating cells in the NBL, a significant fraction of $Ki67^+$ cells should lack pan-cell cycle markers. Ccnd1 is best known for its effects at G1/S but in the retina it is expressed in all phases of the progenitor cell cycle (Barton and Levine, 2008). Indeed, we observed that $Ccnd1^+$ cells were also positive for BrdU, Ccna2, Ccnb2, and PH3; staining was strongest in S-phase nuclei labeled with a pulse of BrdU (30 min) in the inner half of the NBL, and was nuclear or perinuclear in apically located G2/M cells (Fig. 2A, B). Vsx2 is also expressed in progenitors and is required for proliferation of early but not late progenitors (Burmeister et al., 1996; Livne-Bar et al., 2006). In the post-natal retina, Vsx2 is also expressed in bipolar neurons and Müller glia; thus, this marker can be used as an unambiguous progenitor marker only in the embryonic retina (Burmeister et al., 1996; Rowan and Cepko, 2004; Livne-Bar et al., 2006). Indeed, Vsx2 co-localized with BrdU, Ccna2, Ccnb2, and PH3 in the embryonic retina; rich nuclear Vsx2 staining was observed

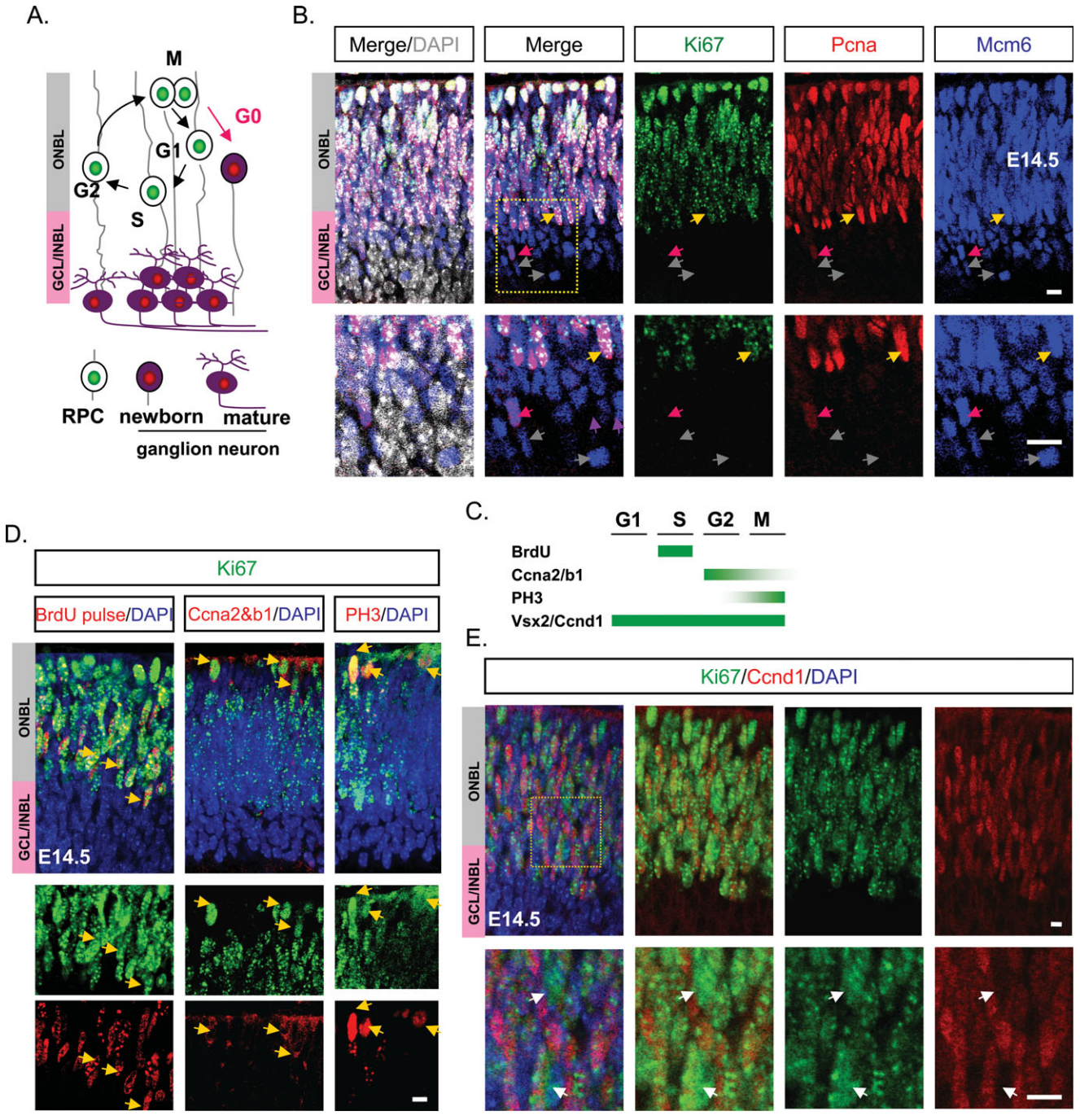

Fig. 1. The expression patterns of Pcna, Mcm6, and Ki67 in the E14.5 WT embryonic retina. **A:** In the NBL, RPCs undergo interkinetic nuclear migration (INM). Thus, S-phase occurs in the middle part of the NBL, M phase at the apical edge, and G1/2 in between. Post-mitotic cells migrate to their final destination and, here, for simplicity, only ganglion cells are shown. **B:** Mcm6 (blue) and to a lesser extent Pcna (red) label cells in both the ONBL and INBL/GCL. In contrast, Ki67 (green) is confined almost exclusively to the ONBL. DAPI (gray) stains cell nuclei. Yellow arrows point to cells co-labeled with all three markers, pink arrows show cells co-labeling with Pcna and Mcm6 but not Ki67, while gray arrows depict cells positive only for Mcm6. **C:** Schematic showing the cell cycle phases marked by the indicated markers. **D:** Ki67 is detectable in all phases of the cell cycle in the WT E14.5 retina. Ki67 (green) co-localizes (yellow arrows highlight examples) with a short 30-min pulse of BrdU (red, S-phase), Ccna2 and b1 (a2 and b1 antibodies were combined; red, G2/M phase), or PH3 (red, M-phase). **E:** All Ccnd1^{+} cells (red) co-localize with Ki67 but some Ki67^{+} cells are Ccnd1^{-} (white arrows). Nuclei in B, D, and E are also stained with DAPI (blue). The boxed regions are at a higher magnification below. ONBL/INBL/GCL: outer neuroblastic layer/inner neuroblastic layer/ganglion cell layer. Scale bars = 10 μm.

in the outer NBL, while a mixture of nuclear and perinuclear staining was observed on the apical surface (Fig. 2A, B).

Having confirmed that Vsx2 and Ccnd1 label all phases of the cell cycle, we analyzed whether there were Ki67 cells that were Vsx2^{-} and Ccnd1^{-}. A notable fraction of Ki67 cells was Vsx2^{-} (e.g., E12.5: 247/3300; 7 ± 0.5%) and a slightly greater fraction was Ccnd1^{-} (e.g., E12.5: 327/

TABLE 1. Antibodies Used to Detect Neuronal Cell Types[a]

Antibody (source)	Species	Target protein	Gene symbol(s)	Cell type(s)	Reference(s)
Novus Biologicals NB300-750	Rabbit	Paired box gene 6	Pax6	Prog, Ga, Am, Ho, Mu	Marquardt et al., 2001; Pan et al., 2008
Chemicon Ab9324	Rabbit	βIII-tubulin	TubbIII (Tuj1)	Ga, Co, subsets of Am, Ho	Sharma and Netland, 2007
Abcam Ab7751	Mouse				
Millipore Ab5054	Rabbit	Calretinin	Calb2	Ga, Am (glycinergic)	Pasteels et al., 1990; Haverkamp and Wassle, 2000; Raymond et al., 2008
Santa Cruz SC-11644	Goat				
Abcam Ab18723	Rabbit	Doublecortin	Dcx	Ga, Am, Ho	Gleeson et al., 1999; Lee et al., 2003
Invitrogen (Molecular Probes) A-21272	Mouse	Elav (embryonic lethal, abnormal vision, Drosophila)-like 2 (Hu antigen B)	Elavl2/3/4 (HuB/C/D)	Ga, Am, Ho	Ekstrom and Johansson, 2003
Abcam ab72354	Sheep	Microtubule associated protein 2	Mtap2 (Map2)	Multiple neurons	Okabe et al., 1989; Bates et al., 1993
Chemicon MAB376	Mouse	Microtubule associated protein 1b	Mtap1b (Map1b, Map5)	Multiple neurons	Bates et al., 1993; Meixner et al., 2000
Chemicon Ab1761	Rabbit	Ubiquitin carboxy-terminal hydrolase L1	Uchl1 (PGP9.5)	Ga, Ho, subsets of Am	Bonfanti et al., 1992; Esteve-Rudd et al., 2010
Chemicon Ab377	Mouse	RNA binding protein, fox-1 homolog (*C. elegans*) 3	Rbfox3 (NeuN)	Ga, Am	Mullen et al., 1992; Wolf et al., 1996; Raymond et al., 2008

[a]Prog: progenitors; Ga: ganglion cells; Am: amacrine cells; Ho: horizontal cells; Co: cones; Mu: Müller glia.

3,300; 9.3 ± 0.2%) (Table 4, Fig. 1E). Consistent with this finding, some $Vsx2^+$ cells were $Ccnd1^-$ (e.g., E12.5: 127/3,000; 4.3 ± 0.2%), but all $Ccnd1^+$ cells were $Vsx2^+$ (Table 5, Fig. 2A), suggesting that Ccnd1 disappears slightly prior to the loss of Vsx2.

The above data are consistent with the notion that some $Ki67^+$ cells in the NBL are post-mitotic differentiating cells rather than progenitors. Alternatively, a significant fraction of $Ki67^+$ progenitors may lack Ccnd1 and more so Vsx2. As noted earlier, all $BrdU^+$ progenitors co-label with Ki67 (Table 3). If ~6–7% of progenitors lack Vsx2 and Ccnd1, one would expect a similar fraction of $BrdU^+$ cells to lack these markers, whereas if these $Ki67^+$ cells are all/mainly post-mitotic then $BrdU^+/Vsx^-$ or $BrdU^+/Ccnd1^-$ cells should be non-existent/rare. In line with the latter model, <1% of $BrdU^+$ progenitors lacked Vsx2 (E12.5: 24/3,000; 0.8 ± 0.1%), and a slightly larger but still very small fraction lacked Ccnd1 (E12.5: 46/3,000; 1.5 ± 0.1%). The G2/M phase cells that we analyzed were always $Vsx2^+$ and $Ccnd1^+$ (Fig. 2B), but because there are so few cells in these phases, it is difficult to exlude the possibility that a tiny fraction lacked Vsx2 and Ccnd1. In summary, while some $Ki67^+/Vsx2^-$ and $Ki67^+/Ccnd1^-$ progenitors, were S-phase progenitors, the fraction (1–1.5%) was too small to explain the entire ~6–7 % of $Ki67^+$ cells that were $Ccnd1^-$ and $Vsx2^-$. We suggest that a minority of $Ki67^+/Vsx2^-/Ccnd1^-$ cells are progenitors that have down-regulated progenitor/cell cycle regulators near the end of their last S-phase prior to cell birth, but that most of these cells are post-mitotic differentiating neurons.

Ki67 Co-Labels Cells Positive for Differentiation Markers

To further test the existence of $Ki67^+$ newborn neurons, we co-labeled embryonic retinas for Ki67 and several established markers expressed in ganglion cells plus other retinal neurons: Tubb3 (Tuj1), Calb2 (Calretinin), Dcx (Doublecortin), Elavl2/3/4 (HuC/D), Map2, Mtap1b (Map1b), Uchl1 (PGP9.5), and Rbfox3 (NeuN). Pax6 labels progenitors and ganglion cells as well as other neurons, and

thus served as a control for double labeling with Ki67 (see Table 1 for cell types and references).

As expected, many Pax6$^+$ cells co-labeled with Ki67 (e.g., E12.5: 45.3 ± 4.9% Pax6$^+$ cells, Fig. 3A, Table 6). Importantly, several neuronal markers also co-labeled Ki67$^+$ cells to varying extents.

For example, at E12.5 Ki67 was detected in 12.4 ± 0.7% Tubb3$^+$ cells, 6.2 ± 1.0% Calb2$^+$ cells, 6.1 ± 0.7% Dcx$^+$ cells, 0.2 ± 0% Elavl2/3/4$^+$ cells, and 0.2 ± 0% Map2$^+$ cells (Fig. 3B–F; Table 6). Ki67 labeling in these cells was often punctate (see higher magnifications in Fig. 3B–F), but this was not unique to neuronal cells, as we also observed punctate Ki67 staining in BrdU$^+$ progenitors (Fig. 1D), and in some neurons Ki67 staining was faint, but clearly positive relative to the negative GCL. This may reflect gradual depletion of Ki67 as neurons differentiate. In contrast to the above neuronal markers, Map1b, Uchl1, and Rbfox3, found only in the forming GCL, never co-localized with Ki67 (Fig. 4, Table 6), indicating that they mark G0 ganglion neurons exclusively. The co-localization of Ki67 with neuronal markers further supports the existence of Ki67$^+$ post-mitotic, differentiating neurons in the NBL. Formally, however, the possibility remained that these differentiation markers are actually induced in progenitors. To address this issue, we next asked whether: (1) Any of the presumed post-mitotic GCL markers co-localize with cell cycle markers other than Ki67, and (2) The timing of Ki67 extinction and differentiation marker induction precedes or follows cell birth.

Multiple Neuronal Proteins Are Not Co-Detected With Cell Cycle Markers Other Than Ki67

We assessed marker detection relative to BrdU (a 30-min pulse), Ccna2, Ccnb1, PH3, Ccnd1, and Vsx2. As expected, a fraction of Pax6$^+$ cells stained for all six progenitor markers (Fig. 5A, Table 6). Unlike Pax6, Tubb3 was not detected in BrdU$^+$ cells, nor was it co-detected with Ccnd1 or Vsx2 (Fig. 5B, Table 6). However, specifically at E12.5 but not later, a minute fraction of Tubb3$^+$ cells co-localized with Ccnb1 (0.05 ± 0.04%) and PH3 (0.1 ± 0.04%) (Fig. 5B, C; Table 6).

In contrast to rare Tubb3 M-phase cells at E12.5, Calb2, Dcx, Elav2/3/4, or Map2 did not co-localize with the six cell cycle markers BrdU (a 30-min pulse), Ccna2, Ccnb1, PH3, Ccnd1, and Vsx2 at this time point or later (Fig. 5C, Table 6). As noted earlier, Map1b, Uchl1, and Rbfox3 were induced after Ki67 is no longer detected (Fig 4), so of the eight differentiation markers tested here, Tubb3 is induced just prior to cell birth at E12.5 but after cell birth at later times, and Calb2, Dcx, Elav2/3/4, Map2, Map1b, Uchl1, and Rbfox3 are always induced after cell birth.

Length of G2/M

To complement the above analyses, we wanted to perform kinetic studies to define when markers are induced relative to the end of S-phase and G2/M. Prior work defined the average length of S-phase and the entire cell cycle at various times during rat retinal development (Alexiades and Cepko, 1996). If the length of G2/M was known, BrdU-labeling could be used to define when markers are extinguished or induced relative to cell birth.

G2/M length is determined by measuring the time necessary to BrdU-label all M-phase cells (here defined by PH3 staining), which is the percentage of labeled mitosis (PLM) method (Quastler and Sherman, 1959). Varying lengths of BrdU chase are used to determine how fast progenitors at the end of S-phase, and thus labeled with the BrdU pulse, reach the end of M-phase. When the chase period after BrdU-labeling is too short, cells that were at the end of S-phase do not reach the end of M-phase and thus some PH3$^+$ cells remain BrdU$^-$, but when the chase period is as long as G2/M all PH3$^+$ cells become BrdU$^+$. We observed that

TABLE 2. Antibodies Used to Detect Cell Cycle Markers

Antibody (source)	Species	Target protein/antigen
Santa Cruz SC-56	Rabbit	PCNA
Santa Cruz SC-9843	Goat	Mcm6
Neomarkers RM-9106S	Rabbit	Ki67
BD Pharmingen 550609	Mouse	Ki67
Abcam Ab1893-125	Sheep	BrdU
Neomarkers MS-1061-S	Mouse	cyclin A2
Neomarkers MS-869-P	Mouse	Cyclin B1
Upstate 06-570	Rabbit	PH3 (Ser10)
Cell Signaling 9706S	Mouse	PH3 (Ser10)
Rod Bremner, Toronto	Sheep	Vsx2

TABLE 3. Ki67 Is Expressed in All Phases of the Cell Cycle[a]

	BrdU pulse$^+$; Ki67$^+$/BrdU pulse$^+$	Ccnb1$^+$;Ki67$^+$/Ccnb1$^+$	PH3$^+$;Ki67$^+$/PH3$^+$	Vsx2$^+$;Ki67$^+$/Vsx2$^+$	Ccnd1$^+$;Ki67$^+$/Ccnd1$^+$
E12.5	3,000/3,000; 100 ± 0%	3,000/3,000; 100 ± 0%	3,000/3,000; 100 ± 0%	3,000/3,000; 100 ± 0%	3,000/3,000; 100 ± 0%
E14.5	3,000/3,000; 100 ± 0%	3,000/3,000; 100 ± 0%	3,000/3,000; 100 ± 0%	3,000/3,000; 100 ± 0%	3,000/3,000; 100 ± 0%
P0	3,000/3,000; 100 ± 0%	3,000/3,000; 100 ± 0%	3,000/3,000; 100 ± 0%	3,000/3,000; 100 ± 0%	3,000/3,000; 100 ± 0%

[a]The percentage of marker$^+$/Ki67$^+$ cells out of the total marker$^+$ population is shown. For example all Ccnd1$^+$ cells were also Ki67$^+$.

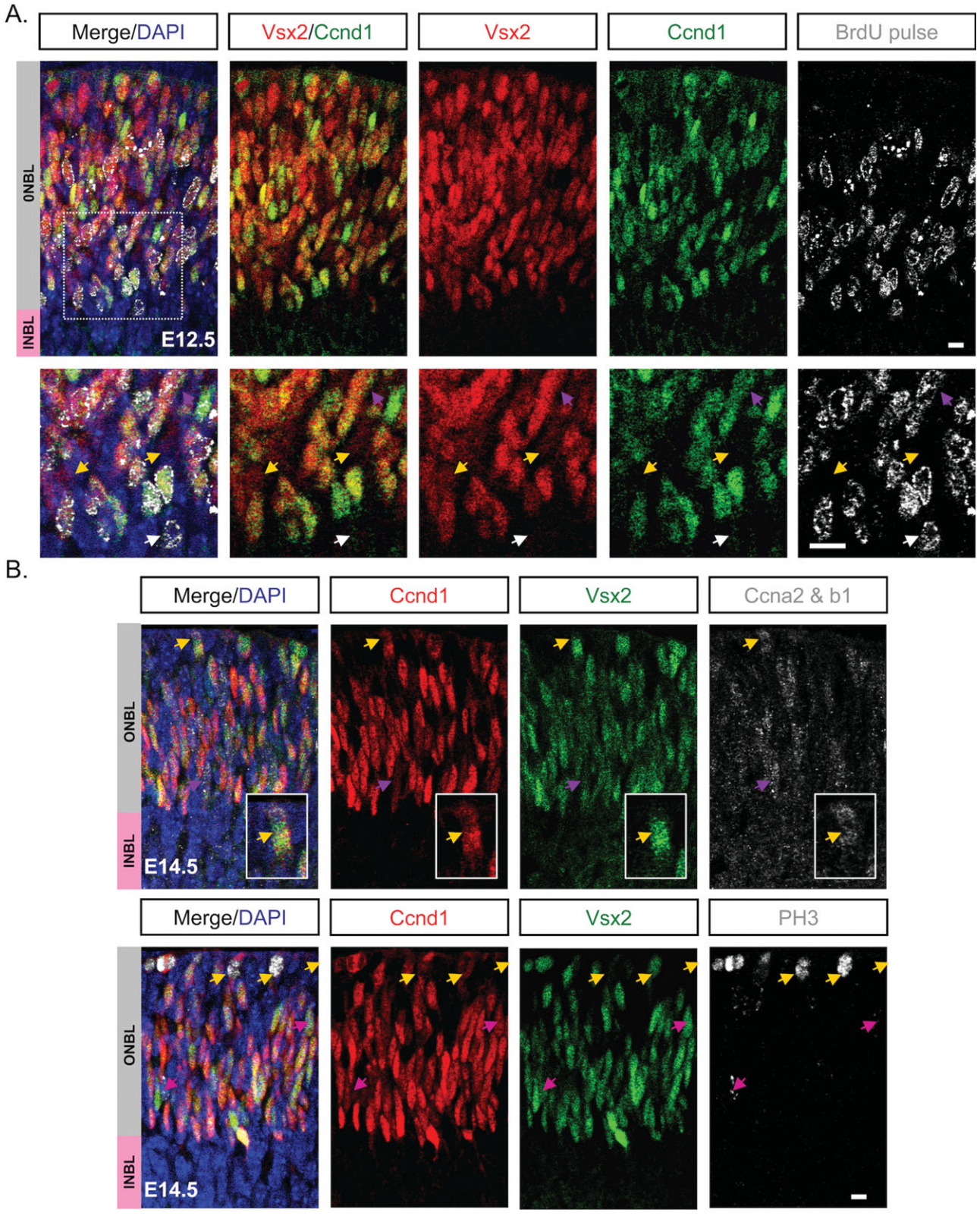

Fig. 2. The expression pattern of Ccnd1 and Vsx2 in the WT embryonic retina. **A:** At E12.5, both Vsx2 (red) and Ccnd1 (green) are expressed throughout the ONBL. The bottom panels are higher magnification of the boxed region. Most cells labeled by a short 30-min BrdU pulse (white) are also Ccnd1$^+$ or Vsx2$^+$ (magenta arrows), but a fraction of S-phase cells lack these markers (white arrows). Further, some Vsx2$^+$ cells lack Ccnd1 (yellow arrows). **B:** At the apical surface both Ccnd1 (red) and Vsx2 (green) co-localize with Ccna2/b1 (a2 and b1 antibodies were combined, white, G2/M phase) or PH3 (white, M-phase). The yellow arrows depict perinuclear Ccna2/b1staining in G2/M cells, or PH3$^+$ M-phase cells, whereas magenta arrows point to sub-apical G2 Ccna2$^+$/b1$^+$ and PH3$^+$ cells. INBL, inner neuroblastic layer; ONBL, outer neuroblastic layer; GCL, ganglion cell layer. Scale bars = 10 μm.

TABLE 4. A Fraction of Ki67$^+$ Cells Lack Vsx2 and/or Ccnd1[a]

	Vsx2$^-$;Ki67$^+$/Ki67$^+$	Ccnd1$^-$;Ki67$^+$/Ki67$^+$
E12.5	247/3,300; 7 ± 0.5%	327/3,300; 9.3 ± 0.2%
E14.5	187/2,950; 6.3 ± 0.1%	187/2,950; 10.3 ± 0.2%
P0	215/3,600; 5.9 ± 0.2%	337/3,600; 9.3 ± 0.2%

[a]The percentage of Ki67$^+$ /Vsx2$^-$ or Ki67$^+$/Ccnd1$^-$ cells out of the total Ki67$^+$ population is shown. Thus, while all Ccnd1$^+$ cells were also Ki67$^+$ (Table 3), not all Ki67$^+$ cells were Ccnd1$^+$.

TABLE 5. A Small Population of Vsx2$^+$ Cells Lack Ccnd1[a]

	Vsx2$^+$;Ccnd1$^-$/Vsx2$^+$	Ccnd1$^+$;Vsx2$^-$/Ccnd1$^+$
E12.5	127/3,000; 4.3 ± 0.2%	0/3,300; 0 ± 0%
E14.5	129/3,000; 4.3 ± 0.1%	0/3,300; 0 ± 0%
P0	132/3,000; 4.4 ± 0.1%	0/3,300; 0 ± 0%

[a]The percentage of Vsx2$^+$ /Ccnd1$^-$ cells out of the total Vsx2$^+$ population, and Ccnd1$^+$/Vsx2$^-$ cells out of the total Ccnd1$^+$ cell population is shown.

in the post-natal retina, it took no less than 30 min post-BrdU injection for cells in the NBL to accumultae enough BrdU to ensure a reproducible detection and quantification. Thus, we considered the start of the chase to be 30 min after BrdU injection at all developmental time points examined. For example, if retinas were harvested 30 or 60 min after the BrdU injection, the time of chase would be 0 or 30 min, respectively. We assessed six chase periods (30, 50, 70, 90, 110, and 130 min) at three embryonic time points (E12.5, 14.5, and 16.5), and eight chase periods (30, 90, 110, 130, 150, 170, 190, and 210 min) at three post-natal time points (P0, P3, and P5). In the embryonic retina at least 90% mitotic cells were BrdU$^+$ after a 70-min chase, which lengthened to 110 min in the post-natal retina (Fig. 6A). In line with live imaging studies indicating that M-phase is ~30 min (Cayouette et al., 2003; Gomes et al., 2011), most PH3$^+$ cells became BrdU$^+$ in a single 20-min chase window (Fig. 6A, Table 7). However, the slope of the labeling curve then flattened and there was a considerable lag between the chase time required to double-label the first ~90% versus the last ~10% of cells, which lengthened across development; 20 min/E12.5, 40 min/E14.5, 60 min/E16.5, and ~100 min post-natally (Fig. 6A, Table 7). These data suggest that a small fraction of progenitors (≤10%) take longer to complete G2 than the bulk of the population. To validate the BrdU/PH3 analyses, we also assessed the fraction of cells that exhibited perinuclear Cyclin B2, which marks late G2. As expected, the fraction of B2$^+$ cells that were BrdU$^+$ slightly exceeded that of PH3$^+$ cells at each time point assessed (Fig. 6B, Table 8). The BrdU chase-PH3 analyses reveal the typical and maximum length of G2/M (Tables 7, 9), and the latter is critical to assess unambiguously whether cell-cycle proteins are detectable after cell birth or, similarly, whether neural markers are induced only after cell birth.

Timing of Ki67 Extinction in Post-Mitotic Cells

Having defined G2/M length, we then applied BrdU pulse-chase analysis to define when Ki67 is extinguished relative to cell birth. Retinas were exposed to a single pulse of BrdU at five developmental stages (E12.4, 14.5, 16.5, P0, 3), and the chase length (i.e., time beyond 30 min of BrdU) necessary to detect the first Ki67$^-$/BrdU$^+$ cells was determined. If Ki67 was extinguished before or after cell birth, a chase period shorter or longer than G2/M would generate Ki67$^-$/BrdU$^+$ cells, respectively. Strikingly, even after an 11.5-h chase period no Ki67$^-$/BrdU$^+$ cells were detected at any of the five developmental time points (Fig. 7A). Only after a 13.5-h chase was a small fraction of Ki67$^-$/BrdU$^+$ cells detected at E12.5 and 14.5, while a 15.5-h chase was needed to detect such cells at E16.6 and P0, and at P3 this was extended to 23.5 h. We confirmed that the Ki67$^-$/BrdU$^+$ cells were differentiating neurons because they co-labeled with Tubb3, which only labels post-mitotic cells from E14.5 and beyond, or Calb2, which always labels post-mitotic neurons (yellow arrows in Fig. 7B). For any single chase period (e.g., 47.5 h), the fraction of Ki67$^-$/BrdU$^+$ cells decreased as development proceeded, indicating that the duration of Ki67 maintenance in post-mitotic cells extends with time. In agreement, at any one developmental time point, the fraction of Ki67$^-$/BrdU$^+$ cells increased with the length of the chase (Fig. 7A). Since the minimal time to extinguish Ki67 after S phase was between 11.5 and 13.5 h in the early embryonic retina or 19.5–23.5 h at P3, and the maximal G2/M is ~1.5 h at E12.5 and ~3.5 h at P3 (Table 9), Ki67 is retained for a minimum of ~10 and 16 h after cell birth, respectively. The actual extent of Ki67 retention at P3 is likely several hours longer than this estimated minimum (>20 h) because the typical (rather than maximal) G2/M is only ~2 h (Table 9), and only a tiny fraction of Ki67$^-$/BrdU$^+$ cells were detected at the 23.5-h chase time (Fig. 7A). For the purposes of discussion, we refer to this period of Ki67 retention in post-mitotic cells in the NBL as G0*.

As noted earlier, Ki67 is detected in the embryonic NBL but disappears as cells begin to emerge into the forming GCL (Fig, 1B, D, E). Thus, as a second approach to approximate the length of G0*, pregnant dams were pulse-labeled with BrdU at E12.5, E14.5, and E16.5, chased for 7.5, 11.5, 23.5, and 47.5 h, and BrdU$^+$/Tubb3$^+$ neurons that had reached the GCL were quantified. The chase time for newborn cells to migrate to the GCL, where Ki67 disappears, was ~11.5 h at E12.5 and E14.5 and between 11.5 and 23.5 h at E16.5 (Fig. 7C), which is similar to the chase times required to

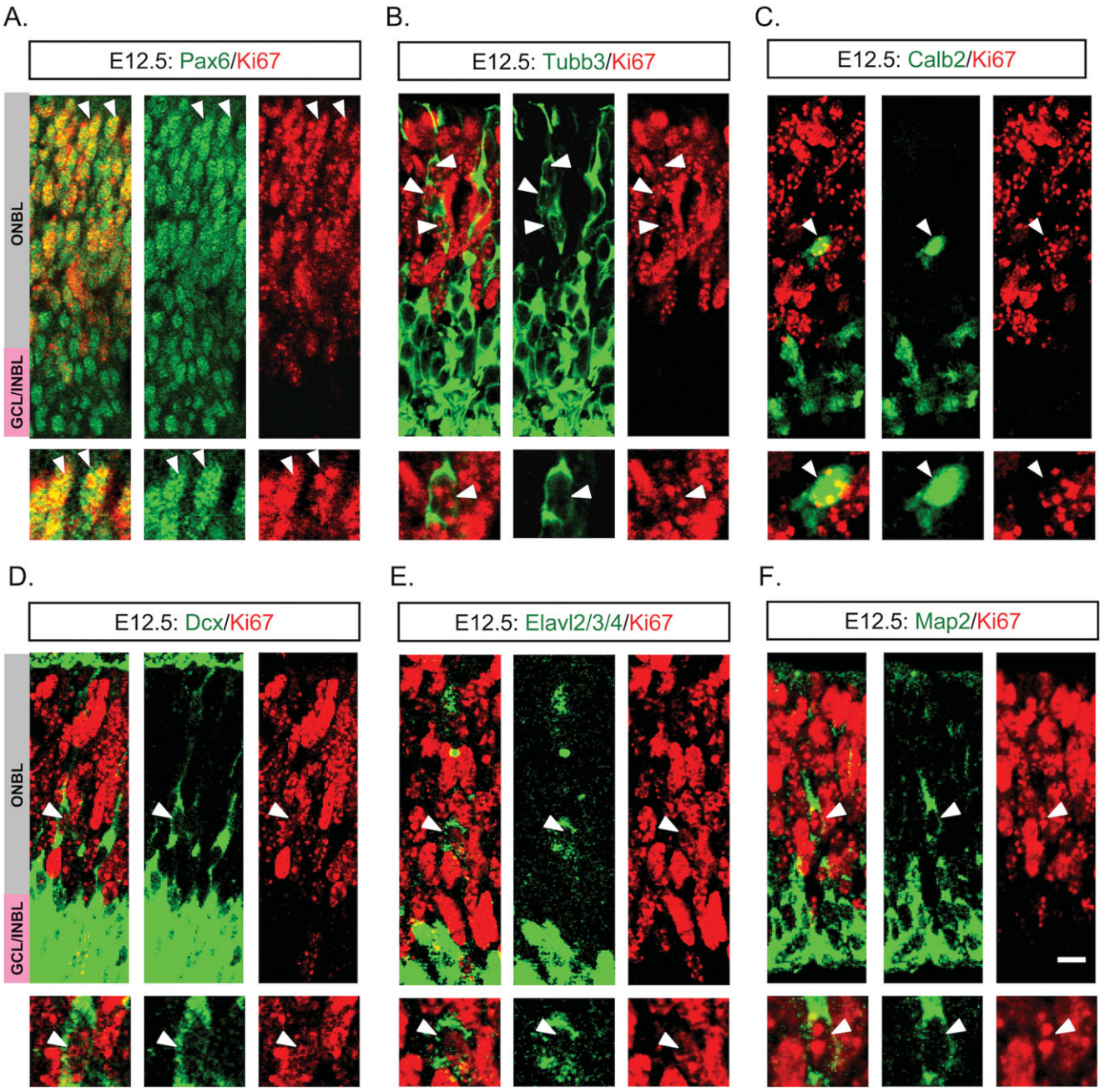

Fig. 3. Ki67 co-localizes with neuronal markers in the embryonic retina. **A:** At E12.5, many Pax6$^+$ cells (green) co-localize with Ki67 (red, white arrows) in the ONBL, and many reside in the INBL/GCL. **B–F:** At E12.5, a subset of Ki67$^+$ cells co-localizes with the neuronal markers Tubb3, Calb2, Map2, Dcx, and Elav2/3/4 (green) in the ONBL (white arrows). INBL, inner neuroblastic layer; ONBL, outer neuroblastic layer; GCL, ganglion cell layer. Scale bars = 10 μm.

observe the first Ki67$^-$/BrdU$^+$ cells (Fig. 7A).

Kinetics of Appearance of GCL Neuronal Proteins

Having defined when Ki67 disappears, we further improved the map of neuronal marker kinetics in the retina by assessing the exact timing of induction of the eight differentiation markers studied earlier: Tubb3, Calb2, Dcx, Elavl, Map2, Map1b, Uchl1, and Rbfox3. As described above, Tubb3 signal appears in a small subset of G2/M progenitors at E12.5 but is restricted to post-mitotic neurons at later times. Consistent with these findings, we found that at E12.5, when typical G2/M is 70 min and maximal G2/M is 90 min, a 30- or 50-min chase did not label Tubb3$^+$ cells, but a 70- or 90-min chase reproducibly detected small proportions (70 min: 0.1 ± 0.04%; 90 min: 0.16 ± 0.0%) of Tubb3$^+$/BrdU$^+$ double-labeled cells (Table 6). The same fraction of Tubb3$^+$ cells colabeled with the G2/M markers Ccnb1 and PH3 (Table 6; Fig. 5B). Thus, multiple pieces of

TABLE 6. Co-Localization of Neuronal Markers With Cell Cycle Proteins and With BrdU After Multiple Chase Periods[a]

Marker/Age	Ki67	BrdU chase (starting 30min after BrdU injection)	Ccnb1	PH3	Vsx2
Pax6	Marker$^+$;Ki67$^+$/Marker$^+$	Marker$^+$;BrdU$^+$/Marker$^+$	Marker$^+$;Ccnb1$^+$/Marker$^+$	Marker$^+$;PH3$^+$/Marker	Marker$^+$;Vsx2$^+$/Marker
E12.5	351/780; 45.3 ± 4.9%	(0m) 200/840; 23.8 ± 1.2%	26/800; 3.25 ± 0.6%	9/800; 1.1 ± 0.6%	950/2,450;38.7±1.2%
Tubb3 (Tuj1)					
E12.5	95/700; 13.5 ± 0.4%	(50m) 0/3,600; 0 ± 0% (70m) 4/3,600; 0.1 ± 0.04% (90m) 6/3,600; 0.16 ± 0.0% (3.5h) 8/3,600; 0.2 ± 0.04% (5.5h) 17/1,200; 0.4 ± 0.04% (11.5h) 33/2,250; 1.4 ± 0.3% (GCL) (23.5h) 377/2,400; 15.7 ± 0.6% (GCL) (47.5h) 560/2,700; 20.7 ± 0.6% (GCL)	2/3,600; 0.05 ± 0.04%	4/3,600; 0.1 ± 0.04%	0/3,600; 0 ± 0%
E14.5	106/800; 13.2 ± 0.5%	(90m) 0/2,100; 0 ± 0% (130m) ½,100; 0.04 ± 0.0% (3.5h) 2/2,100; 0.09 ± 0.0% (5.5h) 5/1,800; 0.2 ± 0.1% (7.5h) 7/2,100; 0.3 ± 0.0% (9.5h) 10/2,100; 0.4 ± 0.0% (11.5h) 8/2,700; 0.29 ± 0.06% (GCL) (23.5h) 52/4,500; 1.15 ± 0.3% (GCL) (47.5h) 450/6,000; 7.5 ± 0.5% (GCL)	0/3,600; 0 ± 0%	0/3,600; 0 ± 0%	0/3,600; 0 ± 0%
E16.5	95/700; 12.9 ± 0.7%	(3.5h) 0/2,700; 0 ± 0% (5.5h) 2/2,700; 0.07 ± 0.0% (7.5h) 5/2,700; 0.1 ± 0.0% (11.5h) 12/6,000; 0.2 ± 0.05% (GCL) (23.5h) 41/15,000; 0.27 ± 0.3% (GCL) (47.5h) 82/24,000; 0.3 ± 0.03% (GCL)	0/900; 0 ± 0%	0/900; 0 ± 0%	0/900; 0 ± 0%
P0	89/800; 11.1 ± 1%	(7.5h) 0/2,700; 0 ± 0% (9.5h) 13/3,130; 0.4 ± 0.0% (23.5h) 30/4,200; 0.7 ± 0.0% (47.5h) 45/4,200; 1.07 ± 0.07% (71.5h) 63/4,200; 1.5 ± 0.07%	0/900; 0 ± 0%	0/900; 0 ± 0%	0/900; 0 ± 0%
P3	95/700; 11.3 ± 1.4%	(7.5h) 0/2,700; 0 ± 0% (9.5h) 8/3,000; 0.2 ± 0.0% (23.5h) 19/4,200; 0.4 ± 0.04% (47.5h) 44/4,200; 1.04 ± 0.1% (71.5h) 63/4,200; 1.5 ± 0.07%	0/900; 0 ± 0%	0/900; 0 ± 0%	0/900; 0 ± 0%
Calb2 (Calretinin)					
E12.5	36/580; 6.2 ± 1.0%	(3.5h) 0/900; 0 ± 0% (5.5h) 3/1,200; 0.2 ± 0.0% (11.5h) 18/1,200; 1.5 ± 0.2%	0/900; 0 ± 0%	0/900; 0 ± 0%	0/900; 0 ± 0%
E14.5	36/600; 6.0 ± 1.0%	(4h) 0/2,100; 0 ± 0%3.5	0/900; 0 ± 0%	0/900; 0 ± 0%	0/900; 0 ± 0%

(Continues on following page)

TABLE 6. (Continued)

Marker/Age	Ki67	BrdU chase (starting 30min after BrdU injection)	Ccnb1	PH3	Vsx2
		(5.5h) 1/1,900; 0.1 ± 0.1% (11.5h) 3/900; 0.3 ± 0% (23.5h) 8/900; 0.8 ± 0.1%			
E16.5	49/600; 8.1 ± 1.0%	(5.5h) 0/900; 0 ± 0% (11.5h) 5/1,200; 0.4 ± 0.1% (23.5h) 40/1,200; 2.6 ± 0.6%	0/900; 0 ± 0%	0/900; 0 ± 0%	0/900; 0 ± 0%
E18.5	30/788; 3.8 ± 0.3%	(90m) 0/900; 0 ± 0%	0/900; 0 ± 0%	0/900; 0 ± 0%	0/900; 0 ± 0%
P0	20/900; 2.2 ± 0.3%	(90m) 0/900; 0 ± 0%	0/900; 0 ± 0%	0/900; 0 ± 0%	0/900; 0 ± 0%
Dcx (Doublecortin)					
E12.5	37/600; 6.1 ± 0.7%	(3.5h) 0/900; 0 ± 0% (5.5h) 3/1,300; 0.25 ± 0.0% (11.5h) 19/1,200; 1.5 ± 0.3%	0/900; 0 ± 0%	0/900; 0 ± 0%	0/900; 0 ± 0%
E14.5	41/1,200; 3.4 ± 0.3%	(7.5h) 0/2,100; 0 ± 0% (11.5h) 5/1,200; 0.4 ± 0.1% (23.5h) 8/1,200; 0.6 ± 0.1%	0/900; 0 ± 0%	0/900; 0 ± 0%	0/900; 0 ± 0%
E16.5	5/1,200; 0.3 ± 1.0%	(7.5h) 0/900; 0 ± 0% (11.5h) 5/1,500; 0.3 ± 0.1% (23.5h) 6/1,500; 0.4 ± 0.0%	0/900; 0 ± 0%	0/900; 0 ± 0%	0/900; 0 ± 0%
P0	0/1200; 0 ± 0%	(90m) 0/900; 0 ± 0%	0/900; 0 ± 0%	0/900; 0 ± 0%	0/900; 0 ± 0%
Elavl 2/3/4 (Hu B/C/D)					
E12.5	3/1,200; 0.2 ± 0.0%	(5.5h) 0/900; 0 ± 0% (7.5h) 4/1,200; 0.3 ± 0.1% (11.5h) 7/1,200; 0.5 ± 0.1%	0/900; 0 ± 0%	0/900; 0 ± 0%	0/900; 0 ± 0%
E14.5	3/1,200; 0.2 ± 0.0%	(7.5h) 0/2,100; 0 ± 0% (11.5h) 8/1,200; 0.3 ± 0.1% (23.5h) 7/1,200; 0.5 ± 0.1%	0/900; 0 ± 0%	0/900; 0 ± 0%	0/900; 0 ± 0%
E16.5	0/1,200; 0 ± 0%	(90m) 0/900; 0 ± 0%	0/900; 0 ± 0%	0/900; 0 ± 0%	0/900; 0 ± 0%
P0	0/1,200; 0 ± 0%	(90m) 0/900; 0 ± 0%	0/900; 0 ± 0%	0/900; 0 ± 0%	0/900; 0 ± 0%
Map2					
E12.5	3/1,200; 0.2 ± 0.0%	(7.5h) 0/900; 0 ± 0% (11.5h) 6/1,200; 0.5 ± 0.0%	0/900; 0 ± 0%	0/900; 0 ± 0%	0/900; 0 ± 0%
E14.5	3/1,200; 0.2 ± 0.0%	(7.5h) 0/2,100; 0 ± 0% (11.5h) 6/1,200; 0.5 ± 0.0% (23.5h) 8/1,200; 0.6 ± 0.1%	0/900; 0 ± 0%	0/900; 0 ± 0%	0/900; 0 ± 0%
E16.5	3/1,200; 0.2 ± 0.0%	(7.5h) 0/900; 0 ± 0% (11.5h) 3/1,200; 0.2 ± 0.0% (23.5h) 8/1,200; 0.5 ± 0.0%	0/900; 0 ± 0%	0/900; 0 ± 0%	0/900; 0 ± 0%
P0	6/2,700; 0.2 ± 0%	(90m) 0/900; 0 ± 0%	0/900; 0 ± 0%	0/900; 0 ± 0%	0/900; 0 ± 0%
Mtap1b (Map1b)					

(Continues on following page)

TABLE 6. (Continued)

Marker/Age	Ki67	BrdU chase (starting 30min after BrdU injection)	Ccnb1	PH3	Vsx2
E12.5	n/a	(11.5h) 0/2,700; 0 ± 0% (23.5h) 31/580; 5.3 ± 0.7% (47.5h) 150/1,130; 13.2 ± 1.2%			
E14.5	0/900; 0 ± 0%				
E16.5	0/900; 0 ± 0%				
Uchl1 (PGP9.5)					
E12.5	n/a	(11.5h) 0/2,800; 0 ± 0% (23.5h) 37/710; 5.2 ± 0.8% (47.5h) 98/720; 13.6 ± 0.8%			
E14.5	0/900; 0 ± 0%				
E16.5	0/900; 0 ± 0%				
Rbfox3 (NeuN)					
E12.5	n/a	(11.5h) 0/2,700; 0 ± 0% (23.5h) 35/720; 4.8 ± 0.1% (47.5h) 102/720; 14.1 ± 0.8%			
E14.5	0/900; 0 ± 0%				
E16.5	0/900; 0 ± 0%				

[a]The percentage of cells positive for nine neuronal markers and the five cell cycle markers (Ki67, Ccnb1, PH3, Vsx2, and BrdU) are shown. Note that BrdU chase is measured starting 30 min after the BrdU injection; thus when retinas were harvested 30 or 80 min after the BrdU injection the chase is 0 or 50 min, respectively. The markers and developmental stages examined are indicated in the first column; thus for Pax6 at E12.5, in the column labeled Ki67, of 780 $Pax6^+$ cells 351 were also $Ki67^+$. The pale orange and gray panels represent co-localization or no co-localization of neuronal markers with proliferation markers, respectively. n/a, not applicable.

data indicate that Tubb3 protein is translated just before cell birth in E12.5 progenitors. Occasionally, we observed pairs of $PH3^+$ cells, likely undergoing anaphase/telophase (Tram and Sullivan, 2002; Li et al., 2005), of which one or both were $Tubb3^+$ suggesting asymmetric or symmetric division, respectively (Fig. 5B). $Tubb3^+$ cells underwent M-phase with their spindles either horizontal or perpendicular relative to the plane of the tissue (Fig. 5B). Subjectively, it appeared that $Tubb3^+$ progenitors were not restricted to symmetrical or asymmetrical division, or perpendicular or horizontal mitotic spindle planes. Irrespective, these data provide further evidence for the presence of Tubb3 protein in M-phase E12.5 progenitors.

At later developmental time points $Tubb3^+/BrdU^+$ cells were observed after increasingly longer BrdU labeling periods. G2/M is typically 70 min at E14.5, and maximally 110 min at E14.5 and 130 min at E16.5 (Fig. 6, Table 9). The first $Tubb3^+/BrdU^+$ cells born at E14.5 were observed after a 130-min chase (0.04 ± 0.0%), but at E16.5 double-positive cells were first seen after a 5.5-h chase (0.07 ± 0.06%). In the post-natal retina, 9.5 h of labeling was required to detect the first $Tubb3^+/BrdU^+$ cells at P0 (0.4 ± 0.1%) and P3 (0.2 ± 0.05%). The fraction of double-labeled cells rose at longer labeling times, consistent with gradual accumulation of $Tubb3^+$ postmitotic neurons (Table 6).

Our earlier data suggested that Calb2, Dcx, Elavl, and Map2 are induced after cell birth in migrating G0* cells, because they co-localized with Ki67 but not with any of the six other cell cycle markers (Figs. 3C–F, 5C; Table 6). Thus, next we used kinetic studies to further test this conclusion. In the early embryonic retina, a 5.5-h chase was required to observe the first $Calb2^+/BrdU^+$ cells (E12.5: 0.25 ± 0%; E14.5: 0.1 ± 0.1%). At E16.5, the first $Calb2^+/BrdU^+$ cells appeared only after an 11.5-h chase (0.4 ± 0.1%). Thus, at all time points examined, the length of the chase exceeded the length of G2/M, confirming that Calb2 induction occurs after cell birth. Based on maximal or typical G2/M lengths, we estimate that Calb2 is induced between ~2–4 h, and ~3–9 h after cell birth at E12.5/E14.5 and

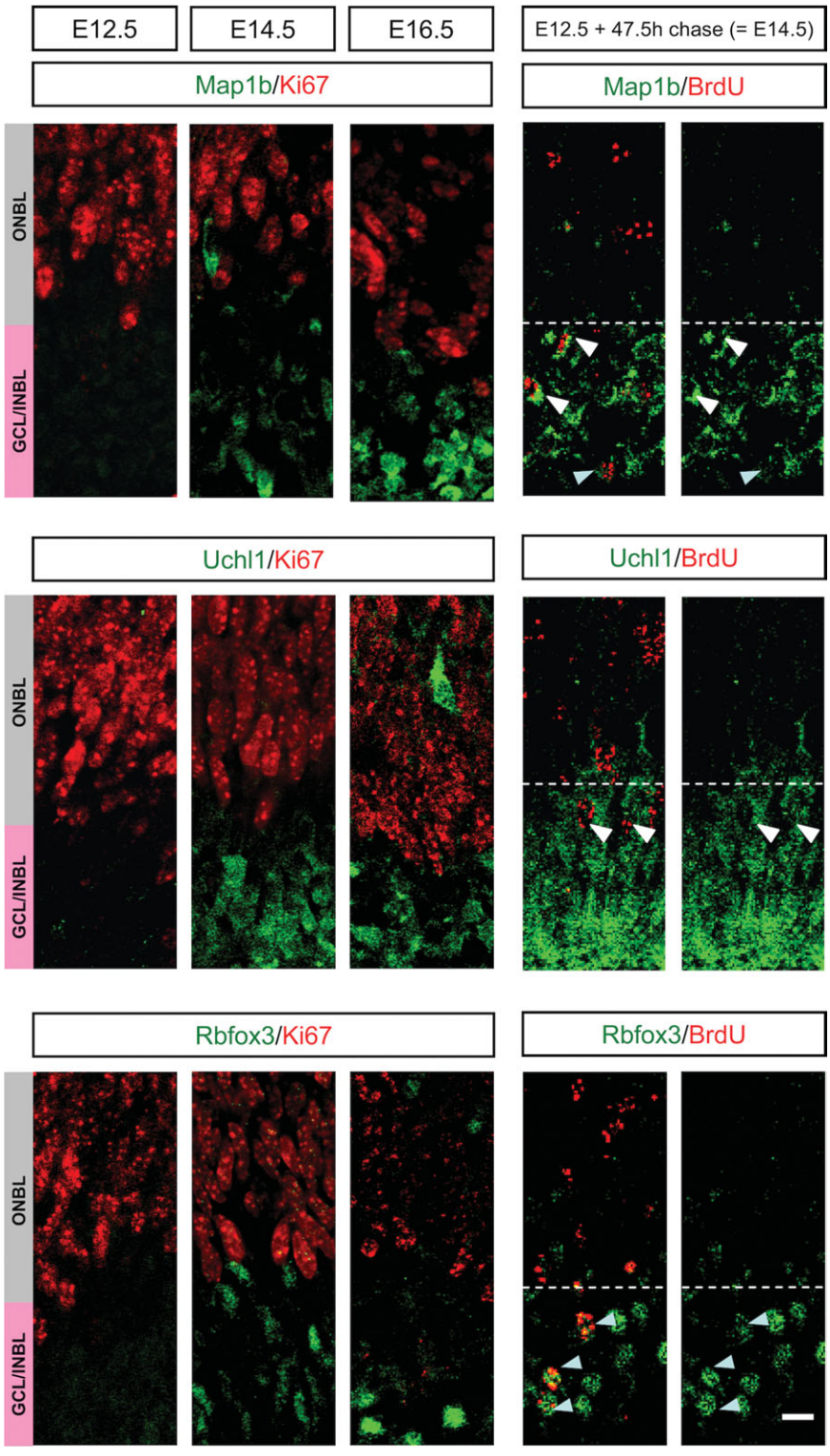

Fig. 4. Map1b, Uchl1, and Rbfox3 are expressed in mature Ki67$^-$ neurons. Map1b, Uchl1, and Rbfox3 (green) appear in the retina after ~E13, labeling ganglion, amacrine, and horizontal cells. These markers never co-localize with Ki67 (red; left panels). Panels on the right show that these neurons require a long chase to become BrdU$^+$ (white arrowheads). The white dotted line marks the boundary between ONBL and INBL/GCL. INBL, inner neuroblastic layer; ONBL, outer neuroblastic layer; GCL, ganglion cell layer. Scale bars = 10 μm.

E16.5, respectively (summarized in Fig. 8). Similarly, we estimate that Dcx was induced 2–4 h after cell birth at E12.5 and ~5.5–10 h at E16.5, respectively; Elavl2/3/4 was induced 4–6 h after cell birth at E12.5 and ~6–10 h at E14.5, respectively (this marker is also induced a few hours after birth in zebrafish retina and hindbrain) (Lyons et al., 2003; Baye and Link, 2007); and Map2 was induced ~5.5–10 h after cell birth at E12.5–E16.5. At P0, we did not perform detailed pulse chase analysis for these markers, but since very few Calb2$^+$ and Map2$^+$ cells or zero Dcx$^+$ or Elav2/3/4$^+$ cells co-localized with Ki67 at this time, we can assume that the timing of their induction is much longer than at embryonic time points (Table 6, Fig. 8).

Map1b, Uchl1, and Rbfox3 never co-localized with Ki67 and were detected in the GCL only after ~E13, arguing that they are induced beyond G0* (Fig. 4). In agreement, only a few BrdU$^+$ neurons expressing Map1b, Uchl1, or Rbfox3 were detected in retinas pulsed with BrdU at E12.5 and chased for 23.5 h, which approximately doubled after another 24 h of labeling (Fig. 4; Table 6). Since, the maximal length of G2/M at E12.5 is 90 min, these markers are detectable in GCL neurons approximately 22 h after the last M-phase.

In summary, these data generate a useful kinetic map of protein appearance in the developing embryonic mouse retina: Thus, the order of detection during the differentiation of GCL neurons is Tubb3 > Calb2 > Dcx > Elavl2/3/4 > Map2 > Map1b, Uchl1, and Rbfox3, and Ki67 is detectable beyond induction of even the very late marker, Map2 (Fig. 8).

DISCUSSION

Cell Cycle Markers in Newborn Migrating Neurons

Our goal was to better define the kinetics with which cell cycle and neuronal proteins are extinguished or induced during cell birth in the developing retina. Neurons in the GCL are post-mitotic, and detection of the pan cell cycle markers Pcna and Mcm6 in this layer stimulated a series of experiments, which revealed that Ki67 is also expressed for an extensive period

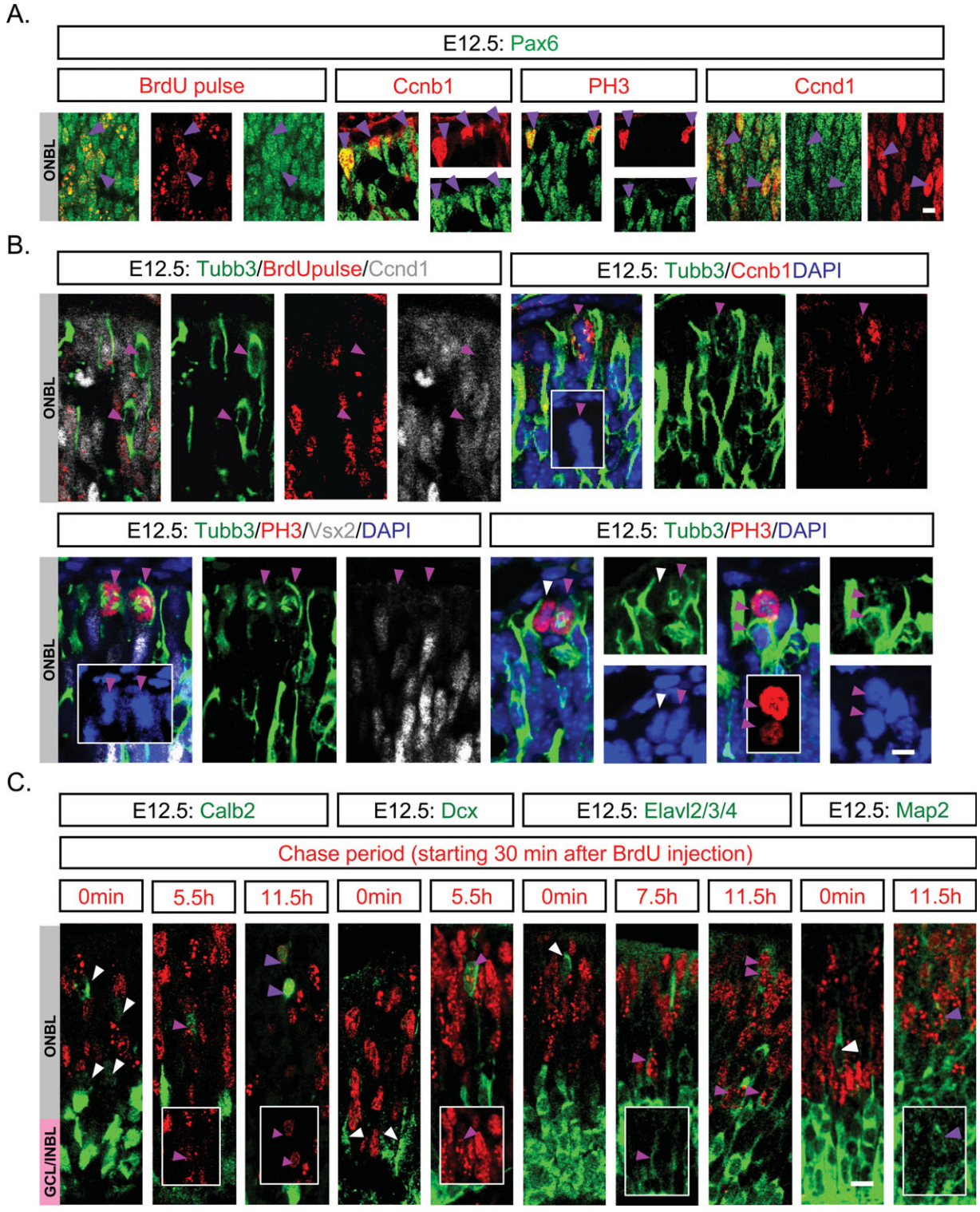

Fig. 5. Induction of retinal differentiation markers. **A:** Pax6^{+} cells (green) are co-labeled (magenta arrows) by a short 30-min pulse BrdU or with Ccnb1, PH3, or Ccnd1 (all red). **B:** At E12.5, Tubb3^{+} cells (green) are not colabeled either with Ccnd1 (white) or a short 30-min BrdU pulse (red) and were weak/negative for Vsx2 (white). However, a minute fraction of Tubb3^{+} cells co-localizes with Ccnb1 and PH3 (red stain, magenta arrows). In some cases, both PH3^{+} cells (red, bottom panels) in a pair were Tubb3^{+} (magenta arrows), whereas in others one was Tubb3^{+} and the other was Tubb3^{-} (white arrow). Nuclei are stained with DAPI (blue). **C:** Calb2, Dcx, Elav2/3/4, or Map2 (green) do not co-localize with a short 30-min pulse (i.e., 0 min chase) of BrdU (red stain, white arrows), but become BrdU^{+} at longer chase times (magenta arrows; see also Table 6). Insets show BrdU or neuronal staining only for highlighted cells. INBL, inner neuroblastic layer; ONBL, outer neuroblastic layer; GCL, ganglion cell layer. Scale bars = 10 μm.

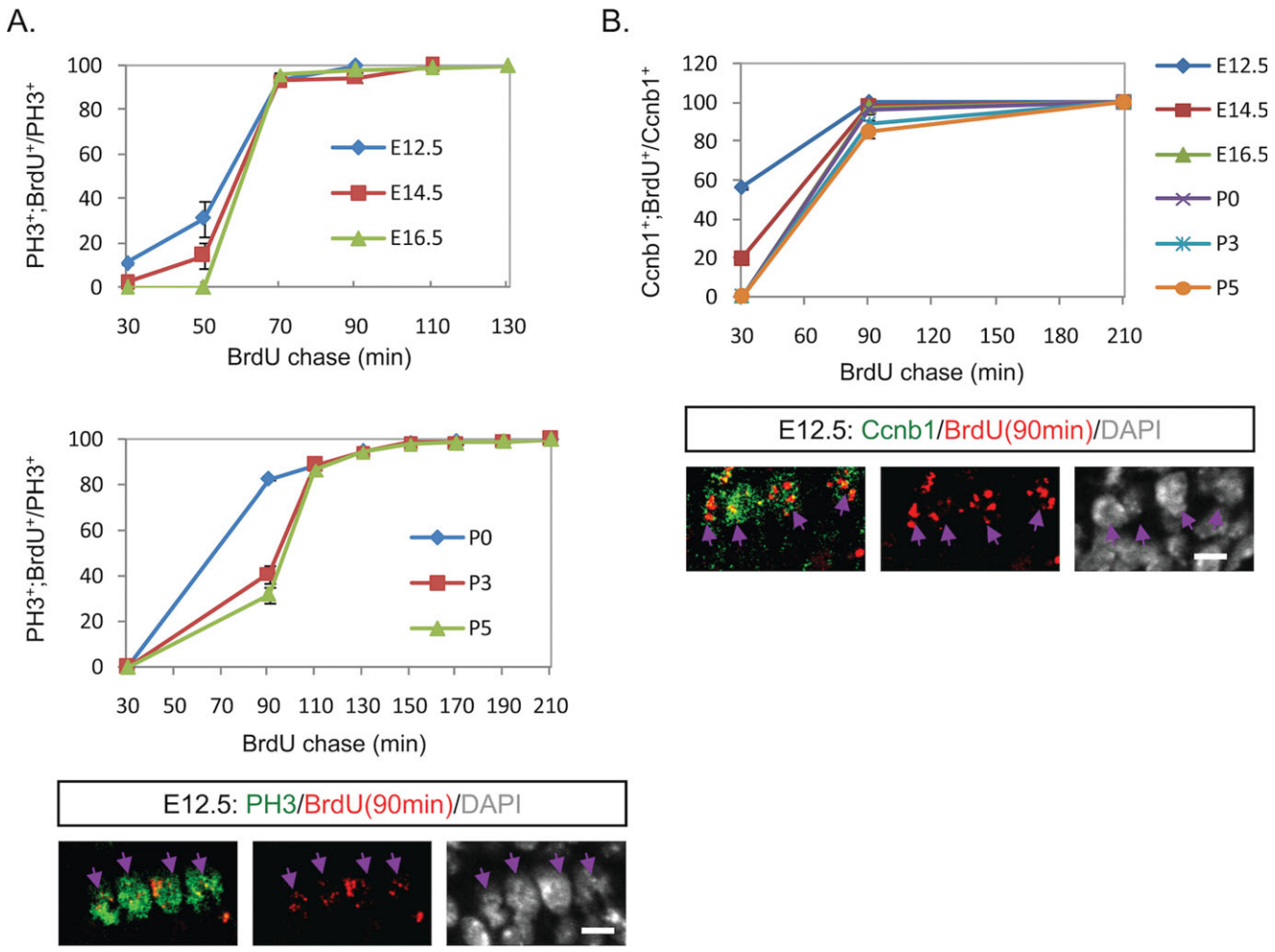

Fig. 6. The length of G2/M. **A:** To measure G2/M, mice of the indicated embryonic (top graph) or post-natal (bottom graph) ages were pulsed with BrdU for 30 min, then chased for the indicated periods (x-axes) and the fraction of all $PH3^+$ cells that was also $BrdU^+$ plotted (y-axes). **B:** As in A, but here the fraction of all $Ccnb1^+$ cells that was $BrdU^+$ was plotted. Images below the graphs in A and B show cells double labeled (magenta arrows) with PH3 or Ccnb1 (green) and BrdU (red); nuclei were labeled with DAPI (white). Scale bars = 10 μm.

TABLE 7. Proportion of BrdU-Labeled $PH3^+$ Cells After Indicated Lengths of BrdU Chase[a]

	$PH3^+;BrdU^+/PH3^+$ (%)					
Chase (min)	E12.5	E14.5	E16.5	P0	P3	P5
30	11.1 ± 0.4	2.1 ± 0	0 ± 0	0 ± 0	0 ± 0	0 ± 0
50	31.2 ± 7.8	14.2 ± 5.7	0 ± 0	n/a	n/a	n/a
70	93.6 ± 0.5	93.2 ± 2.0	96.0 ± 1.3	n/a	n/a	n/a
90	100 ± 0	94.7 ± 2.1	97.9 ± 0.8	82.6 ± 0.6	41.1 ± 3.7	0 ± 0
110		100 ± 0	99.0 ± 1.0	88.6 ± 1.2	88.6 ± 1.6	88.3 ± 1.5
130			100 ± 0	94.5 ± 0.5	94.1 ± 0.2	94.3 ± 2.0
150				98.0 ± 0.3	98.5 ± 0.3	97.6 ± 0.5
170				98.8 ± 0.5	98.5 ± 0.3	98.3 ± 0.7
190				99.4 ± 0.1	99.3 ± 0.2	98.8 ± 0.0
210				100 ± 0	100 ± 0	100 ± 0

[a]n/a, not applicable.

beyond cell birth. We found that 6–7% of $Ki67^+$ cells in the NBL lack other progenitor/cell cycle markers, including Vsx2 (Chx10), BrdU, PH3, and Cyclins D1, A, and B. Moreover, $Ki67^+$ cells were positive for many neuronal proteins, none of which ever co-localized with any of the six other markers of dividing progenitors.

TABLE 8. Proportion of BrdU-Labeled Ccnb1$^+$ Cells After the Indicated Chase Times

	Ccnb1$^+$;BrdU$^+$/Ccnb1$^+$ (%)					
Chase (min)	**E12.5**	**E14.5**	**E16.5**	**P0**	**P3**	**P5**
30	56.5 ± 0.5	20.2 ± 1.8	0 ± 0	0 ± 0	0 ± 0	0 ± 0
90	100 ± 0	97.6 ± 0.7	97.3 ± 0.7	96.3 ± 1.6	89.0 ± 2.5	84.7 ± 2.4
210		100 ± 0	100 ± 0	100 ± 0	100 ± 0	100 ± 0

TABLE 9. G2/M Length at Six Different Developmental Stages[a]

Age	Typical G2/M (~90% BrdU$^+$;PH3$^+$/PH3$^+$ cells) (min)	Maximum G2/M (100% BrdU$^+$;PH3$^+$/PH3$^+$ cells) (min)
E12.5	70	90
E14.5	70	110
E16.5	70	130
P0	110	210
P3	110	210
P5	110	210

[a]Typical and Maximum is defined by the chase time needed to BrdU-label ~90% or 100% PH3$^+$ cells, respectively.

To better map neuronal marker kinetics, we deduced the length of G2/M across retinal development and coupled that information with BrdU-pulse labeling to time the activation of neuronal markers and disappearance of Ki67. Of the differentiation markers assessed here, Tubb3 was induced first. At E12.5, it was detected in M-phase cells, but was induced post-mitotically at later times, rising to ~4–6 h at P0 and ≥ 7.5 h at P3. Calb2 (Calretinin) and Dcx were induced at ~2–4 h after birth at E12.5, rising to ~3.5–9.4 h at E16.5. Elavl2/3/4 was induced 4–6 h after cell birth at E12.5 and 6–10 h at E14.5, respectively. Map2 was induced at least ~5–10 h after birth, while Map1b, Uchl1, and Rbfox3 were induced at ~10–22 h post M-phase. Remarkably, Ki67 co-labeled cells with Tubb3, Calb2, Dcx, Elavl2/3/4, and Map2, but not with Map1b, Uchl1, and Rbfox3, and, in agreement, kinetic analysis showed that Ki67 was not extinguished until 10–22 h after cell birth (Fig. 8).

These data show that, at least in early born cell types, the timing of induction of retinal neuronal markers relative to mitosis extends as development proceeds. However, in rat retina the rod photoreceptor marker rhodopsin is induced 8.5 to 12.5 days after cell birth before E19, but 5.5–6.5 days after cell birth at older ages (Morrow et al., 1998). Potentially, proteins induced soon (<1 day) versus very late (>5 days) after cell birth have different induction kinetics, or alternatively there are cell-specific patterns of expression. Our study focused on early born cells, and further work is required to define the timing with which early markers are induced in rods and other late born cell types.

Several results indicated that Ki67 extinction coincides with the arrival of neurons at their final destination in the GCL. First, Ki67 was detected in the NBL, and only very occasional Ki67$^+$ cells could be seen in the outermost margin of the GCL. Second, the timing of Ki67 extinction was the same as that required for BrdU pulse-labeled neurons to reach the GCL. And third, while Ki67 was co-expressed with the eight neuronal markers discussed above, it was never found together with Map1b, Uchl1, or Rbfox3, which were induced when cells reached the GCL. The DNA replication licensing factor Ctd1 is also expressed in post-mitotic CNS neurons, but unlike Ki67 it remains on even in neurons that reached the GCL and thus could not distinguish G0* and G0 cells (Sakaue-Sawano et al., 2008). It will be interesting to test whether a general molecular switch exists that triggers Ki67 loss at the time when neurons arrive at their final destination.

In summary, our data show that Ki67, like Pcna and Mcm6, is not unique to progenitors, but is present in post-mitotic differentiating neurons in the early embryonic retina and only disappears once cells reach the GCL ~0.5–1 day later.

Implications of Ki67 Presence Beyond Cell Birth

We utilize the term G0* here to facilitate discussion of Ki67$^+$ and Ki67$^-$ post-mitotic neurons, but could G0* and G0 represent distinct functional states? Their physical separation (NBL vs. GCL in the case of neurons studied here), warrants further consideration of this possibility. The retinoblastoma protein, Rb, which binds and represses the E2f family of transcriptional activators, is required to ensure that newborn differentiating retinal neurons exit the cell cycle, and *Rb* null neurons exhibit unscheduled division (Chen et al., 2004; MacPherson et al., 2004). However, Rb inactivation in mature neurons does not trigger cell cycle re-entry (Slack et al., 1998), suggesting that there is a developmental window during which this co-repressor acts to silence cell cycle regulators. In theory, G0* may mark this critical period. Intriguingly, Ki67, Pcna, and Mcm6 are all known E2F targets (Ishida et al., 2001; Bracken et al., 2004), and ectopic division in the *Rb* null retina is E2f1-dependent (Chen et al., 2007). It should be feasible to utilize Ki67 together with neuronal markers such as Calb2 to specifically mark and purify G0* cells, and thus to study the genome-wide kinetics of E2f-target silencing in this population. It would also be

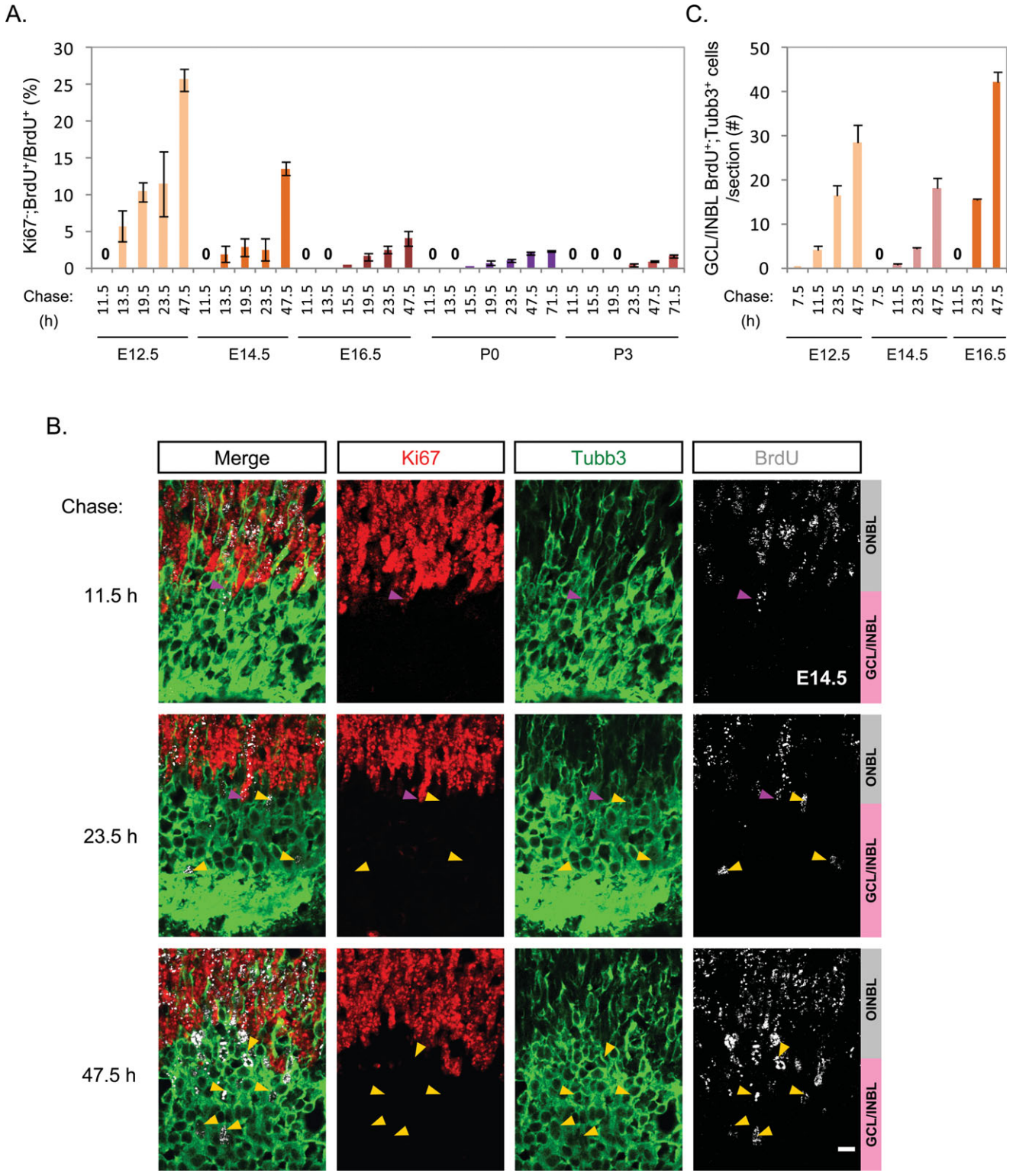

Fig. 7. The timing of Ki67 extinction. **A:** Mice were exposed to BrdU for 30 min at the five indicated developmental stages, retinas harvested after the indicated chase periods (x-axis), and the fraction of $BrdU^+$ cells that were also $Ki67^-$ calculated (y-axis). **B:** Examples of the staining used to generate the data in A. $Tubb3^+$;$BrdU^+$ neurons are shown that are $Ki67^+$ (magenta arrows) or $Ki67^-$ (yellow arrows). **C:** Mice were exposed to BrdU for 30 min at the three indicated developmental stages, retinas harvested after the indicated chase periods (x-axis), and the number of $BrdU^+$;$Tubb3^+$ neurons per section that were in the INBL/GCL cells was plotted (y-axis). INBL, inner neuroblastic layer; ONBL, outer neuroblastic layer; GCL, ganglion cell layer.

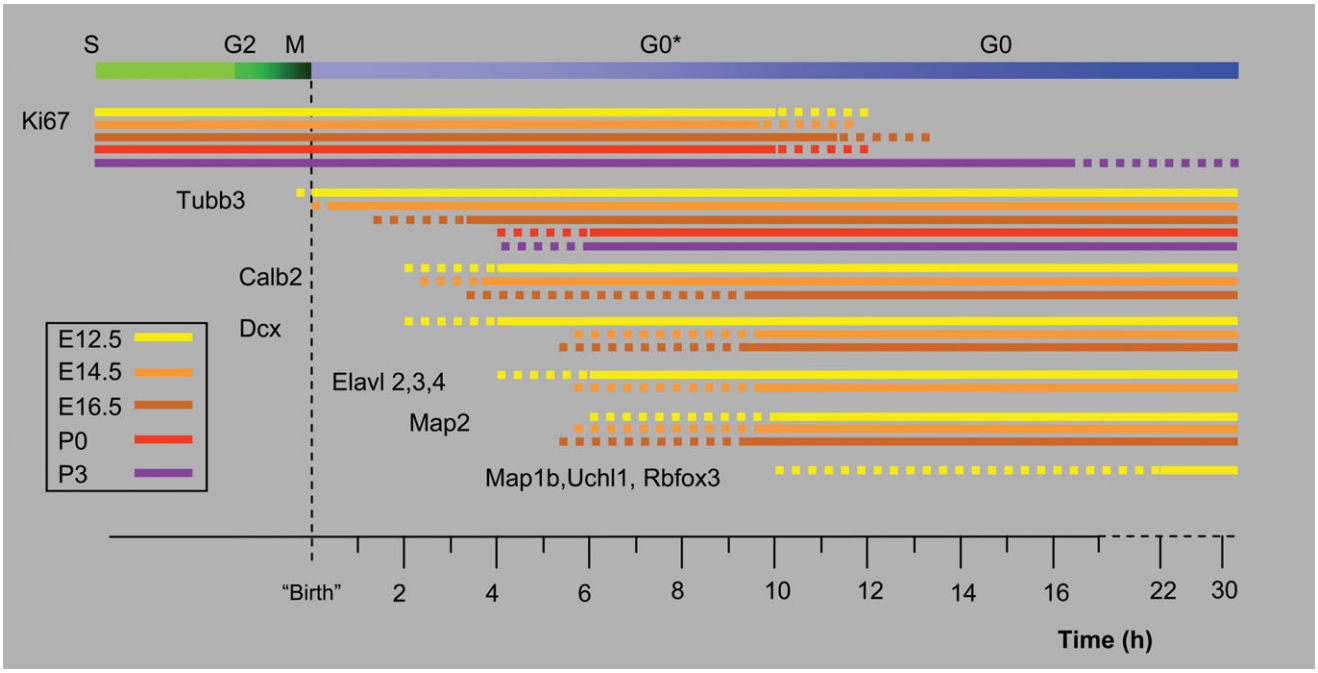

Fig. 8. **A:** Summary of Ki67 extinction and neuronal marker induction in the developing mouse retina. The yellow, orange, brown, red, and magenta lines represent the timing of expression of the indicated markers for cells born at E12.5, E14.5, E16.5, P0, and P3. Not every marker was assessed at all developmental time points. The dotted portion of each coloured line spans the two measured time points between which Ki67 was extinguished or the indicated neuronal markers were induced. Time lines were calculated by subtracting maximum G2/M length (Table 9) from BrdU chase periods (Table 6 for neuronal marker induction, Fig. 7A for Ki67 extinction).

intriguing to determine the kinetics of Ki67, Pcna, and Mcm6 disappearance in E2f-deficient retina (Chen et al., 2009). In situ hybridization will be required to determine if Ki67, Pcna, and Mcm6 mRNA is present as well as protein in post-mitotic neurons. The half-life of Ki-67 protein in cultured cells is only 60–90 min (Bruno and Darzynkiewicz, 1992; Heidebrecht et al., 1996), and it was detectable in differentiating retinal neurons for up to a day, raising the possibility that post-mitotic cells continue to express Ki67 mRNA. The expression of both Pcna and Mcm6 mRNAs in ganglion and amacrine neuronal populations supports this possibility (Trimarchi et al., 2008).

It will also be important to examine whether post-mitotically expressed Ki67 is functionally relevant. Its presence may simply reflect the last vestages of cell cycle gene expression. However, a growing list of studies has demonstrated that cell cycle proteins serve post-mitotic, cell cycle-independent functions that include neuronal migration, axonal growth, synaptic maturation and plasticity (Frank and Tsai, 2009). For example, we reported cell cycle-independent roles of Rb and E2f3a in the differentiation of starburst amacrine cells in the mouse retina (Chen et al., 2007). Ki67 is a commonly used marker in proliferating cells, yet surprisingly little is known about its function. The *Ki67* gene is located on the human chromosome 10 and mouse chromosome 7 (Schonk et al., 1989; Fonatsch et al., 1991). Two alternatively spliced mRNA species encode two isoforms of the protein: a larger isoform (359 kD) and a smaller isoform (320 kD) (Gerdes et al., 1983; Schluter et al., 1993). Inhibiting Ki67 activity with antisense oligonucleotides or blocking antibodies leads to cell cycle arrest in cultured cells (Schluter et al., 1993; Starborg et al., 1996). Further, antisense oligonucleotides reduce proliferation and tumor growth in bladder and renal carcinoma xenograft models (Kausch et al., 2003, 2004, 2005). Interestingly, antisense-treated cell lines and tumors display high levels of apoptosis, suggesting that Ki67 promotes survival as well as cell cycle progression. Ki67 interacts with heterochromatin protein 1 (HP1) proteins suggesting that it may be involved in the control of higher-order chromatin structure (Scholzen et al., 2002).

Ki67 also has a role in the nucleolus where it is directly associated with rRNA genes and is required for their expression (Bullwinkel et al., 2006; Rahmanzadeh et al., 2007). Intriguingly, $Ki67^{+}$ nucleolar spots were reported in post-mitotic as well as dividing cells (Bullwinkel et al., 2006), which is, to our knowledge, the only other study where Ki67 detection has been reported in non-dividing cells. These authors noted that staining could be easily distinguished in post-mitotic cells versus proliferating cells, as it was punctate, confined to very few spots, and nucleolar in the former, but much broader and nuclear in the latter. We did not find this distinction in the developing retina, as we could detect Ki67 in regions outside the nucleolus of post-mitotic cells. Thus distinguishing $Ki67^{+}$ progenitors versus G0* cells required double-labeling with cell cycle or neuronal markers. These varied post-mitotic expression patterns likely reflect distinct Ki67 distribution in differentiat*ing* cells, which we studied, versus

mature, fully differentiated cells assessed in Bullwinkel et al. (2006).

Finally, our study raises a technical concern regarding the use of Ki67, Pcna, and/or Mcm6 to prove definitively that a cell is dividing. Positive staining supports such a deduction because the vast majority of $Ki67^+$ cells in the dividing retina are progenitors. However, proof that a cell is mitotic requires labeling with other cell-cycle markers. This will be particularly pertinent when unscheduled division of neurons is the topic of interest. It is important to note that at any one time in mouse retinal development only a few percent of $Ki67^+$ cells are not progenitors (6–7% of $Ki67^+$ cells lacked the progenitor marker Vsx2), and this fraction is only slightly higher for Pcna or Mcm6. Therefore, with a small correction, these remain valuable markers to approximate the total fraction of dividing cells.

Variable Length of G2/M Among the Retinal Population

Increase in the length of G1 has been associated with promoting cell cycle exit and differentiation in the CNS; however, whether the cell cycle kinetics are the cause or consequence of neuronal progenitor fate decisions is still debated (Gotz and Huttner, 2005; Dehay and Kennedy, 2007; Wilcock et al., 2007; Lange and Calegari, 2010; Arai et al., 2011). Whether G2/M length also affects progenitor fate is also of interest. The percentage of labeled mitoses (PLM) paradigm (Quastler and Sherman, 1959) has been used to measure the length of G2/M in the murine brain, e.g., (Takahashi et al., 1995). Previous rodent retinal cell cycle length studies did not directly measure G2/M, but rather total cell cycle and S-phase length (Denham, 1967; Gloor et al., 1985; Young, 1985b; Alexiades and Cepko, 1996). Employing PLM, we observed that progenitors pass through G2/M in two waves; first, >90% M-phase progenitors becomes BrdU-labeled fast and then the remaining population takes much longer. For example, in the embryonic retina, it took ~1 h to label ~90% progenitors, then another full ~1 h to label the remaining 10%. This data suggests the existence of a small population of progenitors passing slowly through G2/M. Live cell imaging indicates that M phase occurs relatively fast (~30 min) (Cayouette et al., 2003; Gomes et al., 2011), therefore the prolonged labeling of mitotic cells likely reflects variable G2 length. In prior cumulative labeling studies, the time needed to label approximately 90% of progenitors was equivalent to the time needed to label the remaining progenitors (Denham, 1967; Young, 1985b; Alexiades and Cepko, 1996), supporting the notion of a slow dividing RPC population. Recent in vivo imaging data further confirm this idea. Thus, while cultured rat E20 retinal progenitors had a mean cell-cycle length of 56 h, a few percent of the population exhibited much longer cycle times, including some well over 100 h (Gomes et al., 2011). In the zebrafish retina, which develops much faster than in rodents, there is also great heterogeneity in cell cycle length (Baye and Link, 2007; Leung et al., 2011). For example, in the embryonic retina (28–32 h post-fertilization) progenitors spend anywhere between 4–11 h in the cell cycle (Baye and Link, 2007). Live imaging of distinct phases of the cell cycle using a PCNA-GFP fusion protein showed that the G1 and S are the most variable cell cycle phases, but while G2 was on average 40 min, 2/32 (6.7%) of the cells assessed took twice this time to transit G2 (Leung et al., 2011). The latter data are reminiscent of our finding that a similar fraction of progenitors takes twice as long as the majority to complete G2/M in mouse retina (Fig. 6A).

What may be the purpose of a short versus a long G2? As noted above, lengthening of G1 has been associated with earlier cell birth. However, a recent study of the embryonic chick spinal cord found that shortened G2, linked to high levels of CDC25B, promoted neurogenic divisions (Peco et al., 2012). In *Xenopus* retina, Shh shortens both G1 and G2 by down-regulating G2/M regulators such as cdc25c, and cyclins A2 and B1, and leads to precocious cell cycle exit (Locker et al., 2006). Thus, it will be important to determine, for example using in vivo imaging, whether RPCs that exhibit a longer G2/M in mouse retina exhibit any preference for neurogenic or proliferative divisions, and to define the signals that govern G2 length.

EXPERIMENTAL PROCEDURES

Mice

Timed pregnant C57BL/6 (Jackson Labs, Bar Harbor, ME) mice were used for all experiments. Noon of the day the vaginal plug was observed was considered E 0.5. All mice were treated in accordance with institutional and national guidelines. At least three different mice from at least three different litters were used to generate all data.

BrdU Labeling

Mice were injected I.P. with 10 mg/ml BrdU in PBS (Roche, Nutley, NJ) in PBS at 10 mg/kg of body weight. BrdU was detected using the antigen retrieval protocol described below for immunostaing (10 mM sodium citrate, pH 6.0, boiled for 30 min).

Immunostaining

Eyes or whole embryos were fixed in 4% PFA for 24 h, dehydrated in 30% sucrose for 24 h, frozen and cryo-sectioned to 15-μm thickness on Superfrost plus slides (VWR), on a Leica cryostat. Slides were dried for ~4 h at room temperature and either frozen or, if used right away, re-hydrated and washed in PBST (PBS, 0.05% Tween). Slides were immersed in 10 mM sodium citrate (pH 6.0) in coplin jars and boiled for 15–30 min (e.g., anti-protein antibodies required a 15-min boil, while anti-BrdU antibody required a 30-min boil). Sections were cooled to room temperateure (~30 min) and blocked in 4% serum (depending on the species of 2° antibody) in PBS-T for 1 h at RT. Primary antibodies (Tables 1 and 2) were diluted in PBST and kept on the sections for 12 h at 4°C. Secondary antibodies (Alexafluor, Invitrogen, Carlsbad, CA) were diluted in PBST containing a concentration of 200 ng/ml DAPI (Sigma, St. Louis, MO) and kept on sections for 1 h at room

temperature. Slides were washed in ample volumes of PBST between primary and secondary antibodies. Slides were mounted with MOWIOL (Calbiochem, San Diego, CA).

Imaging and Cell Counts

Images were taken with a Zeiss (Thornwood, NY) laser confocal system and were handled with Image J (Sigma filter, z-stack manipulation) and Adobe Photoshop (image cropping, rotation, final overall intensity adjustment). All quantifications (except see below) were performed on the central (i.e., the most mature) part of the retina on a given retinal section. All figures thus represent a typical part of the retina used for scoring. Care was taken to score as many cells as possible (hundreds, sometimes thousands) to ensure statistical significance. For G2/M measurements (i.e., data in Fig. 6 and Tables 7 and 8), several hundred $PH3^+$ and $Ccnb1^+$ cells were scored for each time point throughout the whole section; however, only sections immediately surrounding the optic nerve were used. Note that lack of staining does not automatically mean the absence of expression, but may be the result of epitope-masking or low efficiency of detection. We tried several different staining conditions and when available different types and species of antibodies. We opted to use antigen retrieval for all of the staining presented in this study to minimize the effect of epitope masking.

ACKNOWLEDGMENTS

We thank Michel Cayouette and Pierre Mattar for helpful comments. This study was supported by funds to R.B. from the Canadian Institutes for Health Research, and the Foundation Fighting Blindness Canada.

REFERENCES

Alexiades MR, Cepko C. 1996. Quantitative analysis of proliferation and cell cycle length during development of the rat retina. Dev Dyn 205:293–307.

Arai Y, Pulvers JN, Haffner C, Schilling B, Nusslein I, Calegari F, Huttner WB. 2011. Neural stem and progenitor cells shorten S-phase on commitment to neuron production. Nat Commun 2:154.

Barton KM, Levine EM. 2008. Expression patterns and cell cycle profiles of PCNA, MCM6, cyclin D1, cyclin A2, cyclin B1, and phosphorylated histone H3 in the developing mouse retina. Dev Dyn 237:672–682.

Bates CA, Trinh N, Meyer RL. 1993. Distribution of microtubule-associated proteins (MAPs) in adult and embryonic mouse retinal explants: presence of the embryonic map, MAP5/1B, in regenerating adult retinal axons. Dev Biol 155: 533–544.

Baye LM, Link BA. 2007. Interkinetic nuclear migration and the selection of neurogenic cell divisions during vertebrate retinogenesis. J Neurosci 27: 10143–10152.

Bonfanti L, Candeo P, Piccinini M, Carmignoto G, Comelli MC, Ghidella S, Bruno R, Gobetto A, Merighi A. 1992. Distribution of protein gene product 9.5 (PGP 9.5) in the vertebrate retina: evidence that immunoreactivity is restricted to mammalian horizontal and ganglion cells. J Comp Neurol 322: 35–44.

Bracken AP, Ciro M, Cocito A, Helin K. 2004. E2F target genes: unraveling the biology. Trends Biochem Sci 29: 409–417.

Bruno S, Darzynkiewicz Z. 1992. Cell cycle dependent expression and stability of the nuclear protein detected by Ki-67 antibody in HL-60 cells. Cell Prolif 25:31–40.

Bullwinkel J, Baron-Luhr B, Ludemann A, Wohlenberg C, Gerdes J, Scholzen T. 2006. Ki-67 protein is associated with ribosomal RNA transcription in quiescent and proliferating cells. J Cell Physiol 206:624–635.

Burmeister M, Novak J, Liang MY, Basu S, Ploder L, Hawes NL, Vidgen D, Hoover F, Goldman D, Kalnins VI, Roderick TH, Taylor BA, Hankin MH, McInnes RR. 1996. Ocular retardation mouse caused by Chx10 homeobox null allele: impaired retinal progenitor proliferation and bipolar cell differentiation. Nat Genet 12:376–384.

Cayouette M, Barres BA, Raff M. 2003. Importance of intrinsic mechanisms in cell fate decisions in the developing rat retina. Neuron 40:897–904.

Chen D, Livne-Bar I, Vanderluit JL, Slack RS, Agochiya M, Bremner R. 2004. Cell-specific effects of RB or RB/p107 loss on retinal development implicate an intrinsically death-resistant cell-of-origin in retinoblastoma. Cancer Cell 5: 539–551.

Chen D, Opavsky R, Pacal M, Tanimoto N, Wenzel P, Seeliger MW, Leone G, Bremner R. 2007. Rb-mediated neuronal differentiation through cell-cycle-independent regulation of E2f3a. PLoS Biol 5:e179.

Chen D, Pacal M, Wenzel P, Knoepfler PS, Leone G, Bremner R. 2009. Division and apoptosis of E2f-deficient retinal progenitors. Nature 462: 925–929.

Dehay C, Kennedy H. 2007. Cell-cycle control and cortical development. Nat Rev Neurosci 8:438–450.

Denham S. 1967. A cell proliferation study of the neural retina in the two-day rat. J Embryol Exp Morphol 18: 53–66.

Drager UC. 1985. Birth dates of retinal ganglion cells giving rise to the crossed and uncrossed optic projections in the mouse. Proc R Soc Lond B Biol Sci 224: 57–77.

Ekstrom P, Johansson K. 2003. Differentiation of ganglion cells and amacrine cells in the rat retina: correlation with expression of HuC/D and GAP-43 proteins. Brain Res Dev Brain Res 145: 1–8.

Endl E, Gerdes J. 2000. The Ki-67 protein: fascinating forms and an unknown function. Exp Cell Res 257:231–237.

Esteve-Rudd J, Campello L, Herrero MT, Cuenca N, Martin-Nieto J. 2010. Expression in the mammalian retina of parkin and UCH-L1, two components of the ubiquitin-proteasome system. Brain Res 1352:70–82.

Fonatsch C, Duchrow M, Rieder H, Schluter C, Gerdes J. 1991. Assignment of the human Ki-67 gene (MK167) to 10q25-qter. Genomics 11:476–477.

Frank CL, Tsai LH. 2009. Alternative functions of core cell cycle regulators in neuronal migration, neuronal maturation, and synaptic plasticity. Neuron 62: 312–326.

Gerdes J, Schwab U, Lemke H, Stein H. 1983. Production of a mouse monoclonal antibody reactive with a human nuclear antigen associated with cell proliferation. Int J Cancer 31:13–20.

Gleeson JG, Lin PT, Flanagan LA, Walsh CA. 1999. Doublecortin is a microtubule-associated protein and is expressed widely by migrating neurons. Neuron 23:257–271.

Gloor BP, Rokos L, Kaldarar-Pedotti S. 1985. Cell cycle time and life-span of cells in the mouse eye. Measurements during the postfetal period using repeated 3H-thymidine injections. Dev Ophthalmol 12:70–129.

Gomes FL, Zhang G, Carbonell F, Correa JA, Harris WA, Simons BD, Cayouette M. 2011. Reconstruction of rat retinal progenitor cell lineages in vitro reveals a surprising degree of stochasticity in cell fate decisions. Development 138: 227–235.

Gotz M, Huttner WB. 2005. The cell biology of neurogenesis. Nat Rev Mol Cell Biol 6:777–788.

Haverkamp S, Wassle H. 2000. Immunocytochemical analysis of the mouse retina. J Comp Neurol 424:1–23.

Heidebrecht HJ, Buck F, Haas K, Wacker HH, Parwaresch R. 1996. Monoclonal antibodies Ki-S3 and Ki-S5 yield new data on the 'Ki-67' proteins. Cell Prolif 29:413–425.

Hendzel MJ, Wei Y, Mancini MA, Van Hooser A, Ranalli T, Brinkley BR, Bazett-Jones DP, Allis CD. 1997. Mitosis-specific phosphorylation of histone H3 initiates primarily within pericentromeric heterochromatin during G2 and spreads in an ordered fashion

coincident with mitotic chromosome condensation. Chromosoma 106: 348–360.
Hinds JW, Hinds PL. 1974. Early ganglion cell differentiation in the mouse retina: an electron microscopic analysis utilizing serial sections. Dev Biol 37: 381–416.
Ishida S, Huang E, Zuzan H, Spang R, Leone G, West M, Nevins JR. 2001. Role for E2F in control of both DNA replication and mitotic functions as revealed from DNA microarray analysis. Mol Cell Biol 21:4684–4699.
Kausch I, Lingnau A, Endl E, Sellmann K, Deinert I, Ratliff TL, Jocham D, Sczakiel G, Gerdes J, Bohle A. 2003. Antisense treatment against Ki-67 mRNA inhibits proliferation and tumor growth in vitro and in vivo. Int J Cancer 105:710–716.
Kausch I, Jiang H, Brocks C, Bruderek K, Kruger S, Sczakiel G, Jocham D, Bohle A. 2004. Ki-67-directed antisense therapy in an orthotopic renal cell carcinoma model. Eur Urol 46:118–124; discussion 124–115.
Kausch I, Jiang H, Ewerdwalbesloh N, Doehn C, Kruger S, Sczakiel G, Jocham D. 2005. Inhibition of Ki-67 in a renal cell carcinoma severe combined immunodeficiency disease mouse model is associated with induction of apoptosis and tumour growth inhibition. BJU Int 95:416–420.
Lange C, Calegari F. 2010. Cdks and cyclins link G1 length and differentiation of embryonic, neural and hematopoietic stem cells. Cell Cycle 9: 1893–1900.
Lee EJ, Kim IB, Lee E, Kwon SO, Oh SJ, Chun MH. 2003. Differential expression and cellular localization of doublecortin in the developing rat retina. Eur J Neurosci 17:1542–1548.
Leung L, Klopper AV, Grill SW, Harris WA, Norden C. 2011. Apical migration of nuclei during G2 is a prerequisite for all nuclear motion in zebrafish neuroepithelia. Development 138:5003–5013.
Li DW, Yang Q, Chen JT, Zhou H, Liu RM, Huang XT. 2005. Dynamic distribution of Ser-10 phosphorylated histone H3 in cytoplasm of MCF-7 and CHO cells during mitosis. Cell Res 15: 120–126.
Livne-Bar I, Pacal M, Cheung MC, Hankin M, Trogadis J, Chen D, Dorval KM, Bremner R. 2006. Chx10 is required to block photoreceptor differentiation but is dispensable for progenitor proliferation in the postnatal retina. Proc Natl Acad Sci USA.
Locker M, Agathocleous M, Amato MA, Parain K, Harris WA, Perron M. 2006. Hedgehog signaling and the retina: insights into the mechanisms controlling the proliferative properties of neural precursors. Genes Dev 20: 3036–3048.
Lyons DA, Guy AT, Clarke JD. 2003. Monitoring neural progenitor fate through multiple rounds of division in an intact vertebrate brain. Development 130:3427–3436.
MacPherson D, Sage J, Kim T, Ho D, McLaughlin ME, Jacks T. 2004. Cell type-specific effects of Rb deletion in the murine retina. Genes Dev 18: 1681–1694.
Marquardt T, Ashery-Padan R, Andrejewski N, Scardigli R, Guillemot F, Gruss P. 2001. Pax6 is required for the multipotent state of retinal progenitor cells. Cell 105:43–55.
Meixner A, Haverkamp S, Wassle H, Fuhrer S, Thalhammer J, Kropf N, Bittner RE, Lassmann H, Wiche G, Propst F. 2000. MAP1B is required for axon guidance and Is involved in the development of the central and peripheral nervous system. J Cell Biol 151: 1169–1178.
Morrow EM, Belliveau MJ, Cepko CL. 1998. Two phases of rod photoreceptor differentiation during rat retinal development. J Neurosci 18:3738–3748.
Mullen RJ, Buck CR, Smith AM. 1992. NeuN, a neuronal specific nuclear protein in vertebrates. Development 116: 201–211.
Okabe S, Shiomura Y, Hirokawa N. 1989. Immunocytochemical localization of microtubule-associated proteins 1A and 2 in the rat retina. Brain Res 483: 335–346.
Pan L, Deng M, Xie X, Gan L. 2008. ISL1 and BRN3B co-regulate the differentiation of murine retinal ganglion cells. Development 135:1981–1990.
Pasteels B, Rogers J, Blachier F, Pochet R. 1990. Calbindin and calretinin localization in retina from different species. Vis Neurosci 5:1–16.
Peco E, Escude T, Agius E, Sabado V, Medevielle F, Ducommun B, Pituello F. 2012. The CDC25B phosphatase shortens the G2 phase of neural progenitors and promotes efficient neuron production. Development 139:1095–-1104.
Prigent C, Dimitrov S. 2003. Phosphorylation of serine 10 in histone H3, what for? J Cell Sci 116:3677–3685.
Quastler H, Sherman FG. 1959. Cell population kinetics in the intestinal epithelium of the mouse. Exp Cell Res 17: 420–438.
Rahmanzadeh R, Huttmann G, Gerdes J, Scholzen T. 2007. Chromophore-assisted light inactivation of pKi-67 leads to inhibition of ribosomal RNA synthesis. Cell Prolif 40:422–430.
Raymond ID, Vila A, Huynh UC, Brecha NC. 2008. Cyan fluorescent protein expression in ganglion and amacrine cells in a thy1-CFP transgenic mouse retina. Mol Vis 14:1559–1574.
Rowan S, Cepko CL. 2004. Genetic analysis of the homeodomain transcription factor Chx10 in the retina using a novel multifunctional BAC transgenic mouse reporter. Dev Biol 271:388–402.
Sakaue-Sawano A, Kurokawa H, Morimura T, Hanyu A, Hama H, Osawa H, Kashiwagi S, Fukami K, Miyata T, Miyoshi H, Imamura T, Ogawa M, Masai H, Miyawaki A. 2008. Visualizing spatiotemporal dynamics of multicellular cell-cycle progression. Cell 132: 487–498.
Schluter C, Duchrow M, Wohlenberg C, Becker MH, Key G, Flad HD, Gerdes J. 1993. The cell proliferation-associated antigen of antibody Ki-67: a very large, ubiquitous nuclear protein with numerous repeated elements, representing a new kind of cell cycle-maintaining proteins. J Cell Biol 123:513–522.
Scholzen T, Endl E, Wohlenberg C, van der Sar S, Cowell IG, Gerdes J, Singh PB. 2002. The Ki-67 protein interacts with members of the heterochromatin protein 1 (HP1) family: a potential role in the regulation of higher-order chromatin structure. J Pathol 196:135–144.
Schonk DM, Kuijpers HJ, van Drunen E, van Dalen CH, Geurts van Kessel AH, Verheijen R, Ramaekers FC. 1989. Assignment of the gene(s) involved in the expression of the proliferation-related Ki-67 antigen to human chromosome 10. Hum Genet 83:297–299.
Sharma RK, Netland PA. 2007. Early born lineage of retinal neurons express class III beta-tubulin isotype. Brain Res 1176:11–17.
Slack RS, El-Bizri H, Wong J, Belliveau DJ, Miller FD. 1998. A critical temporal requirement for the retinoblastoma protein family during neuronal determination. J Cell Biol 140:1497–1509.
Starborg M, Gell K, Brundell E, Hoog C. 1996. The murine Ki-67 cell proliferation antigen accumulates in the nucleolar and heterochromatic regions of interphase cells and at the periphery of the mitotic chromosomes in a process essential for cell cycle progression. J Cell Sci 109:143–153.
Takahashi T, Nowakowski RS, Caviness VS, Jr. 1995. The cell cycle of the pseudostratified ventricular epithelium of the embryonic murine cerebral wall. J Neurosci 15:6046–6057.
Tram U, Sullivan W. 2002. Role of delayed nuclear envelope breakdown and mitosis in Wolbachia-induced cytoplasmic incompatibility. Science 296:1124–1126.
Trimarchi JM, Stadler MB, Cepko CL. 2008. Individual retinal progenitor cells display extensive heterogeneity of gene expression. PLoS ONE 3:e1588.
Wilcock AC, Swedlow JR, Storey KG. 2007. Mitotic spindle orientation distinguishes stem cell and terminal modes of neuron production in the early spinal cord. Development 134:1943–1954.
Wolf HK, Buslei R, Schmidt-Kastner R, Schmidt-Kastner PK, Pietsch T, Wiestler OD, Blumcke I. 1996. NeuN: a useful neuronal marker for diagnostic histopathology. J Histochem Cytochem 44:1167–1171.
Young RW. 1985a. Cell differentiation in the retina of the mouse. Anat Rec 212: 199–205.
Young RW. 1985b. Cell proliferation during postnatal development of the retina in the mouse. Brain Res 353:229–239.